About the Effect of Control on Flutter and Post-Flutter of a Supersonic/ Hypersonic Cross-Sectional Wing

Piergiovanni MARZOCCA*, Liviu LIBRESCU*†
and
Walter A. SILVA‡

* Engineering Science and Mechanics Department, Virginia Polytechnic Institute an d State University, Blacksburg, VA 24061 -0219, USA

and

‡ NASA Langley Research Center, Hampton, VA 23681 -2199, USA.

†Corresponding author

Office:	(540) 231 – 5916	Home:	(540) 953 – 0499
Fax:	(540) 231 – 4574	Email:	librescu@vt.edu

Running Title: About the Effects of Control on Flutter and Post-Flutter Instability of Cross-Sectional Wing

About the Effect of Control on Flutter and Post-Flutter of a Supersonic/Hypersonic Cross-Sectional Wing

Piergiovanni Marzocca* and Liviu Librescu†

Virginia Polytechnic Institute and State University, Blacksburg, VA 24061-0219,

and

Walter A. Silva‡

NASA Langley Research Center, Hampton, VA 23681-2199

Abstract

The control of the flutter instability and the conversion of the *dangerous* character of the flutter instability boundary into the *undangerous* one of a cross-sectional wing in a supersonic/hypersonic flow field is presented. The objective of this paper is twofold: i) to analyze the implications of nonlinear unsteady aerodynamics and physical nonlinearities on the character of the instability boundary in the presence of a control capability, and ii) to outline the effects played in the same respect by some important parameters of the aeroelastic system. As a by-product of this analysis, the implications of the active control on the linearized flutter behavior of the system are captured and emphasized. The bifurcation behavior of the open/closed loop aeroelastic system in the vicinity of the flutter boundary is studied via the use of a new methodology based on the Liapunov First Quantity. The expected outcome of this study is: a) to greatly enhance the scope and reliability of the aeroelastic analysis and design criteria of advanced supersonic/hypersonic flight vehicles and, b) provide a theoretical basis for the analysis of more complex nonlinear aeroelastic systems.

* Aerospace Engineer, Research Associate

† Professor of Aeronautical and Mechanical Engineering, Department of Engineering Science and Mechanics.

‡ Senior Research Scientist, Senior Aerospace Engineer, Aeroelasticity Branch, Structures Division, Senior Member AIAA.

Introduction

During the evolution of the combat aircraft, dramatic drops of the flutter speed can be experienced. As a result, the aircraft can attain the critical flutter speed and depending on the *nature of the flutter boundary*, i.e. *catastrophic* or *benign*, the aircraft can exhibit dramatic failures or can survive, respectively. At this stage, according to the flight regulations, the flutter speed should be (22 - 25)% larger than the maximum speed the airplane can experience in the dive flight. This large margin of security is imposed, in order to prevent the catastrophic failure of the aircraft, in the event that the flutter speed would be crossed, and based on what was considered until now that its crossing would result in a catastrophic failure of the aircraft. However, as it was shown, the flutter boundary can also be benign, when, in this case, it can be crossed without the occurrence of catastrophic failures.

This suggests the considerable importance of determining the conditions that result in the benign and catastrophic characters of the flutter boundary, and in the development of proper mechanisms able to convert, in an automatic way, the catastrophic flutter boundary into a benign one. These facts emphasize the considerable importance of at least two issues: a) of including in the aeroelastic analysis the various nonlinear effects, on which basis is possible to get a perfect understanding of their implications upon the character of the flutter boundary, and b) the importance of implementing adequate active feedback control methodologies enabling one not only to increase the flutter speed, but convert the catastrophic flutter boundary into a benign one.

The problem of aeroelastic stability in the vicinity of the flutter boundary, for both the lifting surfaces and supersonic panels, is an issue that requires a great deal of research toward understanding the effects of the nonlinear unsteady aerodynamics and structural/physical nonlinearities. Related to this problem, as it was shown in Ref. 1, the various nonlinearities that occur in the aeroelastic governing equations and are of structural (i.e. arising from the kinematical equations[2-7]), physical (arising from the constitutive equations), or coming from the unsteady aerodynamic loads[2,8,9], can render the *flutter boundary* either *catastrophic* or *benign*. In the former case, crossing the flutter boundary results in an explosive failure of the structure, while in the latter case, a monotonous increase of displacements with the increase of the flight speed takes place.

It is well known that, aerodynamic and structural nonlinearities affect the aeroelastic response of the wing and the flutter boundary[1-3,8,9]. Taking in to account these nonlinearities, an understanding of their potential influence on the character of the flutter can be reached.

This paper restricted to a supersonic/hypersonic cross-sectional wing is intended to address these issues.

Due to the practical importance of these problems, a thorough investigation is needed not only to determine whether or not, for the actual geometrical physical and aerodynamical parameters of the structure, the flutter boundary is of a catastrophic nature, but also to be able to convert it, if it is the case, to a benign one.

In the case when, due to the character of considered nonlinearities coupled with that of geometric and physical parameters of the lifting surface, the flutter boundary is catastrophic, an active control mechanism should be implemented as to convert the flutter boundary into a benign one. In this sense, by controlling the aeroelastic response, the active control methodology[3,10-15] is likely to play a powerful role toward avoiding the occurrence of catastrophic failures, toward rendering the flutter boundary a benign one, and the expansion of the flight envelope.

In this paper a general method able to approach both the problem of lifting surfaces flying at supersonic/hypersonic flight speed regimes and that one of panel flutter[1], have been developed. This methodology will permit to identify the nature of the flutter boundary (i.e. benign or catastrophic) that, in contrast to the actual brute methods, is of an analytical nature and include all the factors, starting with the nonlinearities and continuing with all the aeroelastic parameters of the structure. In this context, general conclusions related to this matter can be reached. Moreover, the analytical methodology to address this issue is based on powerful mathematical tools elaborated by famous mathematicians, such as Bautin[16], a disciple of Liapunov, Hopf, etc.

All these elements suggest that, in order to predict the flutter instability boundary and its character, it is vital to efficiently model the unsteady aerodynamics of lifting surfaces associated with the corresponding flight conditions.

It should be noticed, that in spite of the great practical importance, the literature dealing with the problem of the determination of the flutter boundary of sectional-wing and its character in the presence of both physical and aerodynamic nonlinearities in the conditions of the supersonic/hypersonic flight speed in the subcritical flight conditions is quite void of any such results[1].

There are many potential sources of nonlinearities, which can have a significant effect on an aircraft's aeroelastic response. One essential limitation involving the linearized analysis is that it can only provide information restricted to the flight speed at which the aeroelastic instability occurs. Furthermore, the linearized analyses are restricted to cases where the aeroelastic response amplitudes are small. Often this assumption is violated prior to the onset of instability. Thus, to study the behavior of aeroelastic systems in either the post-instability region or near the point of instability, the nonlinearities of a physical geometrical or aerodynamic nature must be accounted for.

Hopf-Bifurcation

The issue of the *character* of the flutter boundary, i.e. *benign or catastrophic*, can be revealed via determination of the nature of the *Hopf-Bifurcation* (i.e. *supercritical* or *subcritical*, respectively) as featured by the nonlinear aeroelastic system[1,17].

A pictorial representation of the behavior of the aeroelastic system in the vicinity of the flutter boundary versus the dimensionless flight speed in terms of the growth of the limit cycles oscillation (LCO) amplitudes is depicted in Figs. 1a and 1b. The curves indicated by 1 and 2 are characteristic to the stable and unstable domains. In these two cases, below the linear flutter speed V_F, the aeroelastic system is stable, whereas above V_F, the system is unstable for any value of the initial conditions. Above V_F in 3 the system tends to the stable LCOs, that is known as *supercritical Hopf-bifurcation* (H-B), identifying an *undangerous flutter boundary*, whereas the curve indicated by 4 characterizes a *subcritical Hopf-Bifurcation* that yields the catastrophic failure of the spacecraft structure. The latter character of the flutter boundary is referred to as *dangerous*. The solid lines 3 and 4 are also known as *pitchfork bifurcations*, whereas the dotted lines identifies the two cases known as *knee-like shape bifurcations* in which a *turning point* is experienced. Moreover, according to the initial conditions, in 3 and 4 the LCOs amplitudes of the system decrease or increase (stable, unstable). In addition, the cases depicted in 5 and 6 are stable and unstable. Due to its highly destructive effects, flutter instability must not occur within and on the boundary of the operating envelope of the flight vehicle. In this sense, the *nonlinear approach* of lifting surfaces of aeronautical and space vehicles permits determination of the conditions under which undamped oscillations can occur at velocities below the flutter speed, (in this case *the flutter boundary is catastrophic*) (case corresponding to curve 3 in Fig. 1), and also of the conditions under which the flight speed can be exceeded beyond the flutter instability, without catastrophic failure (in this case *the flutter boundary is benign*) (curve 4 in Fig. 1). As a by-product of the nonlinear aeroelastic analysis, the flutter speed V_F i.e. the speed for which the undisturbed form of the considered structure ceases to be stable, can be determined via a linear stability analysis of the aeroelastic system.

Loosely speaking, the Hopf-bifurcation theorem[18] stipulates that if the characteristic equations of the linearized system about an equilibrium position exhibit pairs of complex conjugate eigenvalues that cross the imaginary axis as one of the control parameter varies, (in the present case this parameter is the flight speed V), then for the near-critical values of V there are limit cycles close to the equilibrium point. Just how near the critical flutter speed V_F has to be is not determined, and unless a certain rather complicated expression is nonzero, the existence of these limit cycles is only assured exactly at the flutter speed $(V = V_F)$. The sign of the expression determines the stability of the limit cycle, and whether the limit cycle exists for subcritical $(V \geq V_r)$ or supercritical $(V \leq V_r)$ parameter values.

Behavior in the Vicinity of the Flutter Instability Boundary

In this study, the determination of the dangerous/undangerous character of the critical flutter boundary and its control reduces to the determination of the sign of the first Liapunov quantity, for the instability boundaries that correspond to the purely imaginary roots of the characteristic equation. The approach used in Refs. 1 and 2 for the panel flutter, is extended in the present work to the aeroelasticity of nonlinear 2-D lifting surfaces.

The behavior of the general dynamic systems near the boundaries of the stability domains was investigated by Bautin[16] who considered only those portion of boundary of the region of stability for which the characteristic equations exhibits either one root only, or two roots, that are purely imaginary.

Starting with the expression of the first Liapunov quantity $L(V_F)$, pertinent conditions defining the dangerous and undangerous character of the flutter critical boundary can be determined on the basis of the considered nonlinear aeroelastic system. Specifically, from the condition that $L(V_F)$ should satisfy the inequalities $L(V_F) < 0$ and $L(V_F) > 0$, we determine the undangerous and dangerous portions, respectively, of the boundary of the Routh-Hurwitz domain, and implicitly, the influence played by the various nonlinearities included in the system.

In the next developments the first Liapunov quantity $L(V_F)$ corresponding to the nonlinear flutter equations of open/closed loop cross-sectional wing in a supersonic/hypersonic flow field is derived and is used toward determining the conditions that characterize the nature of the flutter stability boundary.

Nonlinear Model of Cross-Sectional Wing Incorporating an Active Control Capability

Toward formulating the open/closed loop aeroelastic theory of cross-sectional wing in a hypersonic flow field both the aerodynamic and physical nonlinearities are included. This is motivated by the fact that these nonlinearities can contribute differently to the character of the flutter boundary. Moreover in the case when, due to the character of considered nonlinearities, the flutter boundary is catastrophic, an active control mechanism will be implemented as to convert the flutter boundary into a benign one.

The open/closed loop aeroelastic governing equations of a cross-sectional wing featuring plunging and twisting degrees of freedom, elastically constrained by a linear translational spring and nonlinear torsional spring, exposed to a supersonic/hypersonic flow field are[19,20]:

$$m\ddot{h}(t)+S_\alpha\ddot{\alpha}(t)+c_h\dot{h}(t)+K_h h(t)=L_a(t), \tag{1}$$

$$S_\alpha\ddot{h}(t)+I_\alpha\ddot{\alpha}(t)+c_\alpha\dot{\alpha}(t)+M_\alpha=M_a(t)-M_C. \tag{2}$$

Herein $h(t)$ is the plunging displacement (positive downward), $\alpha(t)$ is the pitch angle (positive nose up), the superposed dots denote differentiation with respect to time t, m is the structural mass per unit span, S_α is the static unbalance about the elastic axis, I_α is the mass moment of inertia about the elastic axis of the airfoil, c_h and c_α, K_h are the linear plunging and pitching damping and stiffness coefficients, respectively. Moreover, in Eq. 2:

$$M_\alpha=K_\alpha\alpha(t)\pm\delta_S\hat{K}_\alpha\alpha^3(t), \tag{3}$$

represents the overall nonlinear restoring moment, that includes both the linear and the nonlinear stiffness coefficients, K_α and $\hat{K}_\alpha$, respectively.

Within a linear model $(\delta_S = 0)$, M_α would simply be replaced by $K_\alpha \alpha(t)$. The nonlinear coefficient in Eq. (3) can assume positive or negative values. In the former case we deal with a hard physical nonlinearities, while in the latter one with a soft physical ones. Notice that this nonlinearity appears in the present case in the equation relating the restoring moment with the pitch angle and, it has as such the character of a constitutive equation. For this reason, in contrast to the terminology of *structural nonlinearity*, that in the authors' opinion is not proper for this case, herein we are using that of *physical nonlinearity*.

The tracer δ_S that identifies this type of nonlinearities can take the values 1 or 0 depending on whether this nonlinearity is accounted for or discarded, respectively.

The active nonlinear control can be represented in terms of the moment M_C as:

$$M_C = \overline{M}_C \alpha(t) + \delta_C \hat{M}_C \alpha^3(t), \tag{4}$$

where $\overline{M}_C, \hat{M}_C$ are the linear and nonlinear control gains, respectively. Also in this case, within a linear active control methodology the tracer assumes the value $\delta_C = 0$.

As to reduce the aeroelastic governing equations to a dimensionless form, we also define the parameter:

$$B = \hat{K}_\alpha / K_\alpha \, , \tag{5}$$

and the two active control gain parameters:

$$\psi_1 = \overline{M}_C / K_\alpha \, , \tag{6a}$$

$$\psi_2 = \hat{M}_C / K_\alpha \, . \tag{6b}$$

B constitutes a measure of the degree of the nonlinearity of the system and corresponding to $B < 0$ or $B > 0$, the nonlinearities are soft or hard, respectively, while ψ_1, ψ_2 denote the normalized linear and nonlinear gains, respectively.

Let now derive the nonlinear unsteady aerodynamic lift and moment. From Piston Theory Aerodynamics (PTA)[21-23], the pressure on the upper and lower faces of the lifting surface can be expressed as:

$$p(x,t) = p_\infty \left(1 + \frac{\gamma - 1}{2} \frac{v_z}{a_\infty} \right)^{2\gamma/(\gamma-1)} , \tag{7}$$

where the downwash velocity normal to the lifting surface v_z is expressed as[1]:

$$v_z = -\left(\frac{\partial w}{\partial t} + U_\infty \frac{\partial w}{\partial x}\right)\operatorname{sgn} z\,, \tag{8}$$

and

$$a_\infty^2 = \kappa \frac{p_\infty}{\rho_\infty}. \tag{9}$$

Herein p_∞, ρ_∞, U_∞ and a_∞ are the pressure, the air density, the air speed, and the speed of sound of the undisturbed flow, respectively. In addition, κ is the isentropic gas coefficient, ratio of specific heats, under constant pressure and constant volume, respectively ($\kappa = 1.4$ for air), w is the transversal displacement of the elastic surface from its undisturbed state $w(t) = h(t) + \alpha(t)(x - x_{EA})$, and $\operatorname{sgn} z$, assumes the values 1 or -1 for $z > 0$ and $z < 0$, respectively. In addition, $x_{EA} = bx_0$ is the streamwise position of the pitch axis measured from the leading edge (positive aft), whereas b is the half-chord length of the airfoil.

Retaining, in the binomial expansions of (7), the terms up to and including $(v_z/a_\infty)^3$, yields the pressure formula for the PTA in the third-order approximation[2,22]:

$$\frac{p}{p_\infty} = 1 + \kappa \frac{v_z}{a_\infty}\gamma + \frac{\kappa(\kappa+1)}{4}\left(\frac{v_z}{a_\infty}\gamma\right)^2 + \frac{\kappa(\kappa+1)}{12}\left(\frac{v_z}{a_\infty}\gamma\right)^3. \tag{10}$$

Herein the aerodynamic correction factor γ[23]:

$$\gamma = \frac{M_\infty}{\sqrt{M_\infty^2 - 1}}, \tag{11}$$

enables one to extend the validity of the PTA to the entire low supersonic-hypersonic flight speed regime. As mentioned in Ref. 1, Eq. (10) are satisfactory even for $M \geq 2$. It is also important to remark that, Eqs. (7) through (10) are applicable as long as the transformations through compression and expansion may be considered as isentropic, i.e. as long as the shock losses would be insignificant (low intensity waves).

On the other hand, a more general formula for the pressure, obtained from the theory of oblique shock waves (SWT)[24], and valid over the entire supersonic – hypersonic range, can be applied (see Ref. 2, 22, 24, 25):

$$\frac{p}{p_\infty} = 1 + \kappa \frac{v_z}{a_\infty}\gamma + \frac{\kappa(\kappa+1)}{4}\left(\frac{v_z}{a_\infty}\gamma\right)^2 + \frac{\kappa(\kappa+1)^2}{32}\left(\frac{v_z}{a_\infty}\gamma\right)^3 \tag{12}$$

Eqs. (10) and (12) are similar, the only difference occurring in the cubic term. This is explained by the fact that the entropy variation appears in the pressure expansion, beginning from the third-degree terms. In contrast to the previously mentioned formulae, this one, holds valid both for compression prior the shock wave and for expansion (it is being assumed that the shock waves are all the time attached to the sharp leading edge, and that the flow behind these waves remains supersonic). Moreover, Eq. (12) encompasses a number of advantages such as: i) takes into account for the shock losses occurring in the case of strong waves, ii) can be used, in the form derived in Refs. 24, 25, over a larger range of angles of attack $(\alpha \leq 30^{\circ})$ and Mach numbers $(M \geq 1.3)$, and iii) is still valid for Newtonian speed $(M \rightarrow \infty; \gamma \rightarrow 1)$. Comparisons of results depicting the dangerous and undangerous character of the flutter boundary using these two formulae will be presented at the end of this paper. However, as it clearly appears, within the linear stability analysis, the flutter speed evaluated with these two expressions does not exhibit any differences. This is due to the fact that for such an analysis, only the linear terms are retained toward evaluation of the flutter speed, and these ones are identical for both PTA and SWT (see Eqs. (10) and (12)).

The two cubic term coefficients differs by 10% for $\kappa = 1.4$, and so, for a better prediction of the character of the flutter instability boundary, it has to be included (see Ref. 22). Moreover, the SWT, which considers the pressure losses through shock waves, gives more accurate results then the PTA.

The flutter speed vs. flight Mach number obtained from the PTA and SWT including (i.e. extending the flight speed toward low supersonic range), and discarding the correction factor for the speed γ (in the sense of considering $M_{\infty}^{2} >> 1$, and consequently $\gamma \rightarrow 1$) is shown in Fig. 2. In addition, the flutter boundary obtained via the use of the exact supersonic unsteady aerodynamics is depicted on the same figure. In the low supersonic flight speed regime, the PTA and SWT with the corrective term gives a rather good agreement with the supersonic flow theory and so, this correction should be included. At the same time, for higher supersonic Mach flight numbers, the differences in the flutter predictions based upon the indicated aerodynamic theories practically disappear. In the next developments, unless otherwise stated, Piston theory aerodynamics has been applied.

Considering that the flow takes place on both surfaces of the airfoil (with the speed $U_\infty^+ = U_\infty^- = U_\infty$), from the Eqs. (7) – (10) we can express the aerodynamic pressure difference δp as:

$$\delta p\big|_{PTA} = \frac{4q}{M_\infty}\gamma\left[\left(w,_t \frac{1}{U_\infty} + w,_x\right) + \frac{1+\kappa}{12}\gamma^2 M_\infty^2 \left(w,_t \frac{1}{U_\infty} + w,_x\right)^3\right]. \tag{13}$$

Herein, $M_\infty = U_\infty / a_\infty$ is the undisturbed flight Mach number, while $q = \frac{1}{2}\rho_\infty U_\infty^2$ is the dynamic pressure.

Notice that, in Eq. (13) and in the next developments, the cubic nonlinear aerodynamic term will be reduced to the $(w,_x)^3$ only, in the sense that the nonlinear aerodynamic damping will be discarded. There is no clear-cut for the start of the hypersonic flight speed regime. Generally speaking, speeds above Mach-5 are considered hypersonic. This is the speed at which the aerodynamic heating becomes important in aircraft design. Having in view that this effect will not affect the conclusions about the implications of the considered nonlinearities, the effects of the non-uniform temperature field are neglected here.

Next, the nonlinear unsteady aerodynamic lift $L_a(t)$ and moment $M_a(t)$ per unit wing span can be obtained from the integration of the pressure difference on the upper and lower surfaces of the airfoil:

$$L_a(t) = \int_0^{2b} \delta p dx \quad \text{and} \quad M_a(t) = -\int_0^{2b} \delta p (x - x_{EA}) dx. \tag{14a,b}$$

Their nonlinear final expressions can be cast in compact form as:

$$L_a(t) = -\frac{bU_\infty\rho_\infty}{3M_\infty}\gamma\left\{12U_\infty\alpha(t) + \underline{M_\infty^2 U_\infty (1+\kappa)\gamma^2\alpha^3(t)} + 12\left[\dot{h}(t) + (b - x_{EA})\dot{\alpha}(t)\right]\right\}, \tag{15a}$$

$$\begin{aligned} M_a(t) = \frac{bU_\infty\rho_\infty}{3M_\infty}\gamma\Big\{ & 12U_\infty(b - x_{EA})\alpha(t) + \underline{M_\infty^2 U_\infty (b - x_{EA})(1+\kappa)\gamma^2\alpha^3(t)} \\ & + 4\left[3(b - x_{EA})\dot{h}(t) + \left(4b^2 - 6bx_{EA} + 3x_{EA}^2\right)\dot{\alpha}(t)\right]\Big\} \end{aligned} \tag{15b}$$

As a result, the governing equations (1) – (2) considered in conjunction with Eqs. (15a,b) feature the inertial and the aerodynamical types of couplings.

Upon denoting the dimensionless time $\tau = U_\infty t / b$, the system of governing equations, including the control terms, can be cast as:

$$\xi''(\tau) + \chi_\alpha\alpha''(\tau) + 2\zeta_h(\bar{\omega}/V)\xi'(\tau) + (\bar{\omega}/V)^2\xi(\tau) = l_a(\tau), \tag{16}$$

$$\left(\chi_\alpha/r_\alpha^2\right)\xi''(\tau)+\alpha''(\tau)+\left(2\zeta_\alpha/V\right)\alpha'(\tau)+1/V^2\,\alpha(\tau)+\underline{1/V^2\,B\alpha^3(\tau)}=$$
$$=m_a(\tau)-\underline{\underline{\psi_1/V^2\,\alpha(\tau)-\psi_2/V^2\,\alpha^3(\tau)}}, \tag{17}$$

in which $l_a\left(\equiv L_a b/mU_\infty^2\right)$ and $m_a\left(\equiv M_\alpha b^2/I_\alpha U_\infty^2\right)$, denote the dimensionless aerodynamic lift and moment, respectively. These are expressed as:

$$l_a(\tau)=-\frac{\gamma}{12\mu M_\infty}\left\{12\alpha(\tau)+\underline{M_\infty^2(1+\kappa)\gamma^2\alpha^3(\tau)}+12\left[\xi'(\tau)+\left(b-x_{EA}\right)/b\,\alpha'(\tau)\right]\right\}, \tag{18a}$$

$$m_a(\tau)=\frac{\gamma}{12\mu M_\infty}\frac{1}{r_\alpha^2}\left\{12\left(b-x_{EA}\right)/b\,\alpha(\tau)+\underline{M_\infty^2\left(b-x_{EA}\right)/b\,(1+\kappa)\gamma^2\alpha^3(\tau)}\right.$$
$$\left.+4\left[\left(3\left(b-x_{EA}\right)/b\,\xi'(\tau)+\left(4b^2-6bx_{EA}+3x_{EA}^2\right)/b^2\,\alpha'(\tau)\right)\right]\right\} \quad . \tag{18b}$$

Herein, $\xi=h/b$, is the dimensionless plunging displacement, the superposed primes denote differentiation with respect to time τ, $\mu=m/4\rho b^2$ is the dimensionless mass parameter, $\chi_\alpha=S_\alpha/mb$ is the dimensionless static unbalance about the elastic axis E, $r_\alpha=\sqrt{I_\alpha/mb^2}$ is the dimensionless radius of gyration with respect to E, $V\equiv U_\infty/b\omega_\alpha$ is the non-dimensional airspeed parameter, $\overline{\omega}=\omega_h/\omega_\alpha$ is the plunging-pitching frequency ratio, where $\zeta_h\ (\equiv c_h/2m\omega_h)$, $\zeta_\alpha\ (\equiv c_\alpha/2I_\alpha\omega_\alpha)$ are the damping ratios in plunging and pitching, and where $\omega_\alpha\equiv\sqrt{K_h/m}$ and $\omega_\alpha\equiv\sqrt{K_\alpha/I_\alpha}$ are the uncoupled frequencies of the linearized aeroelastic system counterpart in plunging and pitching, respectively. In addition, in the above equations the terms underscored by a single solid and a dashed line identify the aerodynamic and physical nonlinearities, whereas the terms underscored by a double solid line identify the active control terms, respectively.

As previously stated, the conditions of dangerous or undangerous character of the flutter instability boundary were obtained by the use of the Liapunov first quantity $L(V_F)$. This quantity will be evaluated next.

To this end, the system of governing equations is converted to a system of four differential equations in the form[1,2,16]:

$$\frac{dx_j}{d\tau}=\sum_{m=1}^{4}a_m^{(j)}x_m+P_j\left(x_1,x_2,x_3,x_4\right),\quad j=\overline{1,4}\,. \tag{19}$$

For the present case the functions $P_j\left(x_1,x_2,x_3,x_4\right)$ include both the physical, aerodynamic and nonlinear control terms that can be cast as:

$$P_j(x_1,x_2,x_3,x_4)=\sum_{i=1}^{4} a_{ii}^{(j)}x_i^2+2\sum_{\substack{i,l=1\\(i\neq l)}}^{4} a_{li}^{(j)}x_i x_l+\sum_{i=1}^{4} a_{iii}^{(j)}x_i^3+3\sum_{\substack{i,l=1\\(i\neq l)}}^{4} a_{iil}^{(j)}x_i^2 x_l+6\sum_{\substack{i,l,k=1\\(i\neq l\neq k)}}^{4} a_{ilk}^{(j)}x_i x_l x_k \quad (20)$$

Specializing these expressions for our case, the governing equations in state space form can be reduced to:

$$\frac{dx_1}{d\tau}=x_3, \quad (21a)$$

$$\frac{dx_2}{d\tau}=x_4, \quad (21b)$$

$$\frac{dx_3}{d\tau}=a_1^{(3)}x_1(\tau)+a_2^{(3)}x_2(\tau)+\delta_A a_{222}^{(3)}x_2^3(\tau)+\delta_S a_{222}^{(3)}x_2^3(\tau)+\delta_C a_{222}^{(3)}x_2^3(\tau)+a_3^{(3)}x_3(\tau)+a_4^{(3)}x_4(\tau), \quad (21c)$$

$$\frac{dx_4}{d\tau}=a_1^{(4)}x_1(\tau)+a_2^{(4)}x_2(\tau)+\delta_A a_{222}^{(4)}x_2^3(\tau)+\delta_S a_{222}^{(4)}x_2^3(\tau)+\delta_C a_{222}^{(4)}x_2^3(\tau)+a_3^{(4)}x_3(\tau)+a_4^{(4)}x_4(\tau). \quad (21d)$$

where $(\xi=x_1;\alpha=x_2;\xi'=x_3;\alpha'=x_4)$. The linear active control is included in the coefficients $a_2^{(3)}$ and $a_2^{(4)}$, whereas the nonlinear ones are included in the terms accompanying the tracer δ_C. The coefficients of Eqs. (21) are displayed in Appendix A. As it clearly appears from these coefficients, if the streamwise position of the pitch axis coincides with that of the center chord, the nonlinear aerodynamic terms decay in importance, in the sense that the aerodynamic pitching moment vanishes.

Considering the solution of Eqs. (21) under the form $x_j=A_j\exp(\omega t)$, the characteristic equation corresponding to the linearized system counterpart is:

$$\omega^4+p\omega^3+q\omega^2+r\omega+s=0, \quad (22)$$

where:

$$p=\frac{V\gamma\left[4+3x_0^2+6x_0(\chi_\alpha-1)-6\chi_\alpha\right]+3r_\alpha^2(V\gamma+2M_\infty\mu\zeta_\alpha+2M_\infty\mu\bar{\omega}\zeta_h)}{3M_\infty\mu V(r_\alpha^2-\chi_\alpha^2)}, \quad (23a)$$

$$q=\frac{3M_\infty\mu r_\alpha^2\left[M_\infty\mu(1+\bar{\omega}^2+\psi_1)+2\zeta_\alpha(V\gamma+2M_\infty\mu\bar{\omega}\zeta_h)\right]}{3M_\infty^2\mu^2V^2(r_\alpha^2-\chi_\alpha^2)}$$
$$+\frac{V\gamma\left[V(\gamma+3M_\infty\mu-3M_\infty\mu\chi_\alpha)+8M_\infty\mu\bar{\omega}\zeta_h+6M_\infty\mu\bar{\omega}x_0^2\zeta_h-3M_\infty\mu x_0(V+4\bar{\omega}\zeta_h)\right]}{3M_\infty^2\pi^2V^2(r_\alpha^2-\chi_\alpha^2)}, \quad (23b)$$

$$s=\frac{\bar{\omega}^2\left[M_\infty\mu(1+\psi_1)r_\alpha^2+V^2\gamma(x_0-1)\right]}{M_\infty\mu V^4(r_\alpha^2-\chi_\alpha^2)}, \quad (23c)$$

$$r = \frac{3r_\alpha^2\left[2M_\infty\mu\varpi^2\zeta_\alpha + (1+\psi_1)(V\gamma + 2M_\infty\mu\varpi\zeta_h)\right] + V\gamma\varpi\left[3\varpi x_0^2 - 6x_0(\varpi + V\zeta_h) + 2(2\varpi + 3V\zeta_h)\right]}{3M_\infty\mu V^3\left(r_\alpha^2 - \chi_\alpha^2\right)}. \quad (23d)$$

Three of these parameters, namely q, s, and r are dependent of the linear control gain ψ_1. This is important toward determination of the flutter boundary, that becomes function of the control gain. These expressions substantiate in a strong way the previously mentioned statement, that within the present approach, the issues of the control and nature of flutter boundary can be determined in an analytic way.

As a reminder, for steady motion, the equilibrium is stable, in Liapunov's sense, if the real parts of all the roots of the characteristic equation are negative[26]. It is well known that, the analysis of the roots of this equation, leads to the Routh-Hurwitz (R-H) conditions, which define the system parameter bound for the stability of the considered state of equilibrium.

The R-H conditions reduce to the inequalities $p > 0$, $q > 0$, $r > 0$, $s > 0$, and $\Re = pqr - sp^2 - r^2 > 0$. For the aeroelastic stability problems, in which the condition $\Delta_1 = sp/r + p^2/4 > 0$ should be satisfied, the roots of the characteristic equation on the critical flutter boundary, $\Re = 0$, are given by:

$$\omega_{1,2} = \pm ic, \qquad \omega_{3,4} = m \pm in \qquad \text{where} \qquad i = \sqrt{-1}, \qquad (24a)$$

and

$$c^2 = \frac{r}{p}, \qquad m = -\frac{p}{2}, \qquad n^2 = \frac{sp}{r} - \frac{p^2}{4}, \qquad n > 0. \qquad (24b)$$

The first of equation (24a) reveals that the required condition for the application of Hopf bifurcation is fulfilled.

For sufficient small values of the speed V, all the roots of the characteristic equation are in the left hand side half-plane of the complex variable and the zero solution of the system is asymptotically stable. The value $V = V_F$ for which the two roots of the characteristic equations are purely imaginary and the remaining two are complex conjugate and remain also in the left hand side half-plane of the complex variable, is critical and corresponds to the critical flutter velocity.

Remembering that the condition of Hopf-Bifurcation is obtained if the characteristic equation has a pair of purely imaginary roots, then, in order to identify the "undangerous" portions of the stability boundary from the "dangerous" ones is necessary to solve the stability problem for the system of equations in state-space form in the critical case of a pair of pure imaginary roots.

The expression of the boundary of the region of stability $\Re$ for the open/closed loop cross sectional wing in a supersonic/hypersonic flow field is defined by the equation:

$$
\begin{aligned}
\Re = {} & \frac{1}{27M^4V^6\mu^4\left(r_\alpha^2-\chi_\alpha^2\right)^3}\left\{-3M_\infty\mu\varpi^2\left[M_\infty\mu(1+\psi_1)r_\alpha^2-V^2\gamma(x_0-1)\right]\left[3r_\alpha^2(V\gamma+2M_\infty\mu\zeta_\alpha+2M_\infty\mu\varpi\zeta_h)\right.\right.\\
& \left.+V\gamma\left[4+3x_0^2+6x_0(\chi_\alpha-1)-6\chi_\alpha\right]\right]^2-3M_\infty^2\mu^2\left\{3r_\alpha^2\left[2M_\infty\mu\varpi^2\zeta_\alpha+(1+\psi_1)(V\gamma+2M_\infty\mu\varpi\zeta_h)\right]\right.\\
& \left.+V\gamma\varpi\left[4\varpi+3\varpi x_0^2+6V\zeta_h-6x_0(\varpi+V\zeta_h)\right]\right\}^2\left(r_\alpha^2-\chi_\alpha^2\right)+\left\{3r_\alpha^2\left[2M_\infty\mu\varpi^2\zeta_\alpha+(1+\psi_1)\right.\right.\\
& \left.\left.(V\gamma+2M_\infty\mu\varpi\zeta_h)\right]+V\gamma\varpi\left[4\varpi+3\varpi x_0^2+6V\zeta_h-6x_0(\varpi+V\zeta_h)\right]\right\}\left\{3r_\alpha^2(V\gamma+2M_\infty\mu\zeta_\alpha\right.\\
& +2M_\infty\mu\varpi\zeta_h)+V\gamma\left[4+3x_0^2+6x_0(\chi_\alpha-1)-6\chi_\alpha\right]\left\}\right\{3M_\infty\mu r_\alpha^2\left[M_\infty\mu\left(1+\varpi^2+\psi_1\right)\right.\\
& \left.+2\zeta_\alpha(V\gamma+2M_\infty\mu\varpi\zeta)\right]+V\gamma\left[8M_\infty\mu\varpi\zeta_h+6M_\infty\mu\varpi x_0^2\zeta_h-3M_\infty\mu x_0(V+4\varpi\zeta_h)\right.\\
& \left.\left.\left.+V(\gamma+3M_\infty\mu-3M_\infty\mu\chi_\alpha)\right]\right\}\right\}=0
\end{aligned}
\tag{25}
$$

Notice that this expression is general and includes the relationship between the flutter speed and the flutter frequency, parameters evaluated on $\Re=0$ in terms of the basic geometrical and flight parameters. In the particular case in which the structural damping ratios in plunging and pitching are discarded and $\gamma \Rightarrow 1$, i.e. no correction for the flight speed range is included, the expressions of frequency χ_F and speed V_F on the flutter instability boundary can be obtained as:

$$
\chi_F=\left(\frac{\omega_\alpha}{\omega}\right)_F^2=\frac{r_\alpha^2+(1-x_0)^2+\frac{1}{3}-2\chi_\alpha(1-x_0)}{(1+\psi_1)r_\alpha^2+\varpi^2\left[(1-x_0)^2+\frac{1}{3}\right]},
\tag{26}
$$

$$
V_F=\frac{U_F}{b\omega_\alpha}=\frac{\mu M}{\sqrt{\chi_F}}\sqrt{\frac{\chi_\alpha^2-\left(\varpi^2\chi_F-1\right)r_\alpha^2(\chi_F-1)}{\mu M\left[(1+\psi_1)\chi_\alpha+(1-x_0)\left(\varpi^2\chi_F-(1+\psi_1)\right)\right]-\frac{1}{3}(1+\psi_1)}}.
\tag{27}
$$

These expressions, constitute the extended counterparts of those obtained by Ashley and Zartarian[21,23] in the case of absence of the control. As a result, Eqs. (26) and (27) represent the dimensionless flutter frequency and flutter speed of the closed-loop system. As a remark, in these expressions only the linear control gain is involved.

In Fig. 3 the influence of the linear control gain ψ_1 on the flutter speed is emphasized. It clearly appears that with the increase of the control gain, an increase of the flutter speed is experienced. Moreover, toward larger values of ψ_1 the control is more effective and a larger increase in the flutter speed is experienced.

Following the ideas developed by Liapunov[27] – Bautin[16], the dangerous or undangerous portions of the flutter instability boundary can be determined, via determination of the sign of the Liapunov's coefficient. Following Bautin, the system of equations (21) is reduced to the canonical form as:

$$\frac{d\xi_1'}{d\tau} = -c\xi_2' + Q_1(\xi_1', \xi_2', \xi_3', \xi_4'), \tag{27a}$$

$$\frac{d\xi_2'}{d\tau} = c\xi_1' + Q_2(\xi_1', \xi_2', \xi_3', \xi_4') \ , \tag{27b}$$

$$\frac{d\xi_3'}{d\tau} = m\xi_3' - n\xi_4' + Q_3(\xi_1', \xi_2', \xi_3', \xi_4'), \tag{27c}$$

$$\frac{d\xi_4'}{d\tau} = n\xi_3' - m\xi_4' + Q_4(\xi_1', \xi_2', \xi_3', \xi_4'), \tag{27d}$$

where m, n and c are determined by Eqs. (24b). In Eqs. (27) Q_i denote the nonlinear terms appearing in the canonical counterpart of Eqs. (21). The expression of the first Liapunov quantity is given under a closed form in Ref. 1. For the present case, the first Liapunov quantity is expressed in terms of the coefficients $A_{kls}^{(j)}$ as:

$$L(V_F) = \frac{3\pi}{4c}\left(A_{111}^{(1)} + A_{222}^{(2)} + A_{112}^{(2)} + A_{122}^{(1)}\right), \tag{28}$$

where, the terms in the bracket of Eq. (28) are expressed via the coefficients $a_{kls}^{(j)}$ appearing in Eqs. (18), as:

$$A_{kls}^{(j)} = \frac{1}{\Delta_0}\left(\hat{\alpha}_{j3} a_{222}^{(3)} \alpha_{2k} \alpha_{2l} \alpha_{2s} + \hat{\alpha}_{j4} a_{222}^{(4)} \alpha_{2k} \alpha_{2l} \alpha_{2s}\right). \tag{29}$$

The various components of (28), evaluated on the instability boundary are explicitly expressed as:

$$A_{111}^{(1)} = \frac{1}{\Delta_0}\left(\hat{\alpha}_{13} a_{222}^{(3)} + \hat{\alpha}_{14} a_{222}^{(4)}\right)\alpha_{21}^3 , \tag{30a}$$

$$A_{222}^{(2)} = \frac{1}{\Delta_0}\left(\hat{\alpha}_{23} a_{222}^{(3)} + \hat{\alpha}_{24} a_{222}^{(4)}\right)\alpha_{22}^3 , \tag{30b}$$

$$A_{112}^{(2)} = \frac{1}{\Delta_0}\left(\hat{\alpha}_{23} a_{222}^{(3)} + \hat{\alpha}_{24} a_{222}^{(4)}\right)\alpha_{22}\alpha_{12}^2 , \tag{30c}$$

$$A_{122}^{(1)} = \frac{1}{\Delta_0}\left(\hat{\alpha}_{13} a_{222}^{(3)} + \hat{\alpha}_{14} a_{222}^{(4)}\right)\alpha_{12}\alpha_{22}^2 . \tag{30d}$$

where the adjoint of a matrix is defined as $[\hat{\alpha}_{jp}] = \Delta_0 [\alpha_{jp}]^{-1}$ and $\Delta_0 = \|\alpha_{ij}\|$ is the determinant of the matrix of coefficient α_{ij}. In addition, the parameters α_{ij} are:

$$\alpha_{12} = c\begin{vmatrix} a_2^{(2)} & a_4^{(2)} \\ a_2^{(1)} & a_4^{(1)} \end{vmatrix} + c\begin{vmatrix} a_3^{(3)} & a_4^{(3)} \\ a_3^{(1)} & a_4^{(1)} \end{vmatrix}, \tag{31a}$$

$$\alpha_{21} = \begin{vmatrix} a_3^{(3)} & a_1^{(3)} & a_4^{(3)} \\ a_3^{(1)} & a_1^{(1)} & a_4^{(1)} \\ a_3^{(2)} & a_1^{(2)} & a_4^{(2)} \end{vmatrix} - c^2 a_4^{(2)}, \tag{31b}$$

$$\alpha_{22} = c\begin{vmatrix} a_1^{(1)} & a_4^{(1)} \\ a_1^{(2)} & a_4^{(2)} \end{vmatrix} + c\begin{vmatrix} a_3^{(3)} & a_4^{(3)} \\ a_3^{(2)} & a_4^{(2)} \end{vmatrix}, \tag{31c}$$

while the coefficients of the system of Eq. (29) are:

$$\begin{aligned} a_{222}^{(3)} &= (\delta_S B + \delta_C \psi_2)\frac{r_\alpha^2 \chi_\alpha}{V_F^2 (r_\alpha^2 - \chi_\alpha)} - \delta_A \frac{M_\infty (1+\gamma)\lambda^3 \left[(x_0 - 1)\chi_\alpha + r_\alpha^2\right]}{12\mu (r_\alpha^2 - \chi_\alpha)} \\ &= (\delta_S S_{NL} + \delta_C C_{NL})\chi_\alpha - \delta_A A_{NL}\left[(x_0 - 1)\chi_\alpha + r_\alpha^2\right] \end{aligned}, \tag{32a}$$

$$\begin{aligned} a_{222}^{(4)} &= -(\delta_S B + \delta_C \psi_2)\frac{r_\alpha^2}{V_F^2 (r_\alpha^2 - \chi_\alpha)} + \delta_A \frac{M_\infty (1+\gamma)\lambda^3 (x_0 - 1 + \chi_\alpha)}{12\mu (r_\alpha^2 - \chi_\alpha)} \\ &= -(\delta_S S_{NL} + \delta_C C_{NL}) + \delta_A A_{NL}(x_0 - 1 + \chi_\alpha) \end{aligned} \tag{32b}$$

Herein the physical and aerodynamic nonlinear parameters as well the nonlinear control terms are defined as:

$$S_{NL} = B\frac{r_\alpha^2}{V_F{}^2 (r_\alpha^2 - \chi_\alpha)}, \tag{33}$$

$$A_{NL} = \frac{M_\infty (1+\gamma)\lambda^3}{12\mu (r_\alpha^2 - \chi_\alpha)}, \tag{34}$$

$$C_{NL} = \psi_2 \frac{r_\alpha^2}{V_F{}^2 (r_\alpha^2 - \chi_\alpha)} \tag{35}$$

where V_F is the flutter speed. Moreover, δ_A, δ_S and δ_C are tracers that, depending on the effect that are identified, should be taken as one when the respective effect is taken into account, and zero when is discarded.

Defining $\left[\bar{\alpha}_{jp}\right] = \left[\alpha_{jp}\right]^{-1}$ and noticing that $c > 0$, the flutter critical boundary is *undangerous* or *dangerous*, if the following inequalities, $L(V_F) < 0$ and $L(V_F) > 0$, are fulfilled, respectively, where:

$$\begin{aligned} L(V_F) = &\left(\bar{\alpha}_{13} a_{222}^{(3)} + \bar{\alpha}_{14} a_{222}^{(4)}\right)\alpha_{21}^3 + \left(\bar{\alpha}_{23} a_{222}^{(3)} + \bar{\alpha}_{24} a_{222}^{(4)}\right)\alpha_{22}^3 \\ &+ \left(\bar{\alpha}_{23} a_{222}^{(3)} + \bar{\alpha}_{24} a_{222}^{(4)}\right)\alpha_{22}\alpha_{12}^2 + \left(\bar{\alpha}_{13} a_{222}^{(3)} + \bar{\alpha}_{14} a_{222}^{(4)}\right)\alpha_{12}\alpha_{22}^2 . \end{aligned} \tag{36}$$

In an extended form, the above expression can be cast as:

$$
\begin{aligned}
L(V_F) = (\delta_S S_{NL} + \delta_C C_{NL})\big[(\bar{\alpha}_{13}\chi_\alpha - \bar{\alpha}_{14})\alpha_{21}^3 + (\bar{\alpha}_{23}\chi_\alpha - \bar{\alpha}_{24})\alpha_{22}^3 + (\bar{\alpha}_{23}\chi_\alpha - \bar{\alpha}_{24})\alpha_{22}\alpha_{12}^2 + (\bar{\alpha}_{13}\chi_\alpha - \bar{\alpha}_{14})\alpha_{12}\alpha_{22}^2\big] \\
- \delta_A A_{NL}\big\{\{\bar{\alpha}_{13}[(x_0 - 1)\chi_\alpha + r_\alpha^2] - \bar{\alpha}_{14}(x_0 - 1 + \chi_\alpha)\}\alpha_{21}^3 + \{\bar{\alpha}_{23}[(x_0 - 1)\chi_\alpha + r_\alpha^2] - \bar{\alpha}_{24}(x_0 - 1 + \chi_\alpha)\}\alpha_{22}^3 \\
+ \{\bar{\alpha}_{23}[(x_0 - 1)\chi_\alpha + r_\alpha^2] - \bar{\alpha}_{24}(x_0 - 1 + \chi_\alpha)\}\alpha_{22}\alpha_{12}^2 + \{\bar{\alpha}_{13}[(x_0 - 1)\chi_\alpha + r_\alpha^2] - \bar{\alpha}_{14}(x_0 - 1 + \chi_\alpha)\}\alpha_{12}\alpha_{22}^2\big\}
\end{aligned} \quad . (37)
$$

Using the expressions of S_{NL}, A_{NL} and C_{NL} (Eqs. (33) through (35)); from Eq. (37) that is multiplied by $V_F{}^2$, paralleling the procedure devised in Refs. 1 and 2, the character of the flutter boundary, i.e. undangerous or dangerous, may be expressed, respectively, under the concise form as:

$$
V_F{}^2 < V_r{}^2, \quad \text{or} \quad V_F^2 > V_r^2. \tag{38a,b}
$$

where:

$$
V_r{}^2 = A_1 / A_2 . \tag{38c}
$$

In Eq. (38c) the parameter A_1 contains the physical and the nonlinear control gain parameter, whereas A_2, includes the aerodynamical nonlinearities. These are expressed as:

$$
\begin{aligned}
A_1 = \frac{(\delta_S B + \delta_C \psi_2) r_\alpha^2}{(r_\alpha^2 - \chi_\alpha)}\big[(\bar{\alpha}_{13}\chi_\alpha - \bar{\alpha}_{14})\alpha_{21}^3 + (\bar{\alpha}_{23}\chi_\alpha - \bar{\alpha}_{24})\alpha_{22}^3 \\
+ (\bar{\alpha}_{23}\chi_\alpha - \bar{\alpha}_{24})\alpha_{22}\alpha_{12}^2 + (\bar{\alpha}_{13}\chi_\alpha - \bar{\alpha}_{14})\alpha_{12}\alpha_{22}^2\big]
\end{aligned} \quad , \tag{39a}
$$

$$
\begin{aligned}
A_2 = \frac{\delta_A M_\infty (1+\gamma)\lambda^3}{12\mu(r_\alpha^2 - \chi_\alpha)}\big\{\{\bar{\alpha}_{13}[(x_0 - 1)\chi_\alpha + r_\alpha^2] - \bar{\alpha}_{14}(x_0 - 1 + \chi_\alpha)\}\alpha_{21}^3 \\
+ \{\bar{\alpha}_{23}[(x_0 - 1)\chi_\alpha + r_\alpha^2] - \bar{\alpha}_{24}(x_0 - 1 + \chi_\alpha)\}\alpha_{22}^3 \\
+ \{\bar{\alpha}_{23}[(x_0 - 1)\chi_\alpha + r_\alpha^2] - \bar{\alpha}_{24}(x_0 - 1 + \chi_\alpha)\}\alpha_{22}\alpha_{12}^2 \\
+ \{\bar{\alpha}_{13}[(x_0 - 1)\chi_\alpha + r_\alpha^2] - \bar{\alpha}_{14}(x_0 - 1 + \chi_\alpha)\}\alpha_{12}\alpha_{22}^2\big\}
\end{aligned} \quad . \tag{39b}
$$

As a very important consequence, in absence of nonlinear control, for $B < 0$, i.e. for soft physical nonlinearities, the expression of V_r^2 is negative, and the relation $V_F^2 > V_r^2$ is satisfied for any flight supersonic Mach number. This implies that in this case, even in the presence of the linear control, a subcritical Hopf-Bifurcation is experienced, (see Fig. 9, where the Liapunov First Quantity is depicted). On the other hand, for $B > 0$, i.e. for hard physical nonlinearities, in the presence of the linear control, the transition from the undangerous flutter boundary to the dangerous one occurs at higher flight Mach numbers (see, for example Fig. 9).

Moreover, as mentioned before, if $x_0 = 1$, Eq. (37) reduces to the following one:

$$L(V_F) = (\delta_S S_{NL} + \delta_C C_{NL})[(\overline{\alpha}'_{13}\chi_\alpha - \overline{\alpha}'_{14})\alpha_{21}^3 + (\overline{\alpha}'_{23}\chi_\alpha - \alpha'_{24})\alpha_{22}^3 + (\overline{\alpha}'_{23}\chi_\alpha - \alpha'_{24})\alpha_{22}\alpha_{12}^2 + (\overline{\alpha}'_{13}\chi_\alpha - \alpha'_{14})\alpha_{12}\alpha_{22}^2]$$
$$- \delta_A A_{NL}[(\overline{\alpha}'_{13}r_\alpha^2 - \overline{\alpha}'_{14}\chi_\alpha)\alpha_{21}^3 + (\overline{\alpha}'_{23}r_\alpha^2 - \overline{\alpha}'_{24}\chi_\alpha)\alpha_{22}^3 + (\overline{\alpha}'_{23}r_\alpha^2 - \overline{\alpha}'_{24}\chi_\alpha)\alpha_{22}\alpha_{12}^2 + (\overline{\alpha}'_{13}r_\alpha^2 - \overline{\alpha}'_{14}\chi_\alpha)\alpha_{12}\alpha_{22}^2] \quad ,(40)$$

In this case, it clearly appears that a decrease of the influence of the aerodynamic nonlinearities on the aeroelastic system is experienced.

Critical Flutter Boundary: Stability Analysis in Presence of Active Control

As to render clearly the results concerning the critical flutter boundary for open/closed loop cross-sectional wings, as displayed in Figs. 6 through 16, some explanations on a couple of generic plots, Figs. 4a and 4b, are given next. In Fig. 4a, the intersections of the two curves V_F and V_r, separate the parts of the flutter boundary that are undangerous (for $V_F < V_r$) from the dangerous ones, for which the opposite relationship is satisfied, namely $V_F > V_r$. Needless to say, in such a case a switch of the sign in the first Liapunov quantity occurs, (see Fig. 4b). The graph depicting the first Liapunov quantity $L(V_F)$, that defines the portions of the boundary of the region of stability, is displayed in Fig. 4b. On the curves that represent the flutter critical boundary, the "dangerous" and "undangerous" portions are being indicated for each case by the dotted and gross lines, respectively. In the range in which $V_F < V_r$, we have the following possible situations: i) for $V < V_F$, as time unfolds, a decay of the motion amplitude is experienced, which reflects the fact that in this case the subcritical response is involved, ii) an ideal condition, for $V = V_F$ the center limit cycle occurs, which reflects the fact that in this case a periodic orbit is experienced and iii), for the speed parameter $V > V_F$, the response becomes supercritical, while for $V_F > V_r$ the subcritical flutter boundary is experienced. The parameters in use for the simulations, unless otherwise specified, are chosen as:

$\mu = 100; \chi_\alpha = 0.25; \overline{\omega} = 1.2; r_\alpha = 0.5; \zeta_\alpha = \zeta_h = 0; x_0 = 0.5; \gamma = 1; \kappa = 1.4; \delta_A = \delta_S = \delta_C = 1; B = 50$.

The effect of physical nonlinearities on the character of the flutter boundary is carried out in terms of the nonlinear parameter B, see Eq. (4). For the condition indicated, the aeroelastic system appears to be characterized by subcritical Hopf bifurcation in the upper half plane (dangerous flutter boundary) and supercritical in the lower half plane (undangerous flutter boundary). The graph depicting the first Liapunov quantity $L(V_F)$ for uncontrolled lifting surface and for the cases in which aerodynamic and physical hard nonlinearities are retained, is displayed in Fig. 6. In these simulations both types of nonlinearities, have been considered separately and together. It clearly appears that in presence of aerodynamic nonlinearities only, the Liapunov quantity is positive for any flight Mach number. This result reflects the fact that this type of nonlinearities provides a "catastrophic" character to the flutter boundary, implying that a subcritical H-B occurs. On the other hand, in presence of physical hard nonlinearities only the opposite situation is experienced. In this sense, at relatively moderate supersonic flight Mach numbers, the flutter is benign, while with the increase of the flight Mach number, the flutter becomes dangerous. This implies that for larger flight Mach numbers the effects of the aerodynamic nonlinearities become prevalent. It is also shown that the neglect of nonlinear aerodynamic terms, yields inadvertent results related to the character of the flutter instability boundary, especially at high flight Mach numbers, when the aerodynamic nonlinearities become detrimental from the point of view of the character of flutter boundary.

Moreover, as a consequence of these results, if the aerodynamic nonlinearities are discarded $(\delta_A = 0)$ the aeroelastic system features supercriticality or subcriticality for any flight Mach number, depending on whether hard $(B > 0)$ or soft $(B < 0)$ physical nonlinearities are present, respectively.

The influence of the hard physical and aerodynamic nonlinearities for controlled/uncontrolled system is presented in Fig. 7. The dotted and solid lines identify the case in which both physical hard ($B = 50$) and aerodynamical nonlinearities, and aerodynamic nonlinearities only ($B = 0$), are included, respectively. The control mechanism act in both situations toward the stabilization of the system, i.e. to enhance the flutter behavior. Also in this case, the inherent dangerous character of the flutter boundary that corresponds to the case when only aerodynamic nonlinearities are considered, can be converted into a benign one.

Figures 6 and 7 show that the soft nonlinearities contribute to render the system unstable and that only acting with a nonlinear control the inherent catastrophic type boundary can be converted into a benign one (Fig. 6). Moreover, it clearly appears that the linear active control cannot change the character of flutter boundary when soft physical nonlinearities are present (Fig. 7).

From Eq. (28) defining the Liapunov quantity, the supercritical parts of the flutter boundary are defined in a closed form. Moreover, by using Eqs. (37), curves associated with V_F and V_r have been plotted in Figs. 10, 12, 14 for $B = 50$ and $\delta_A = 1$. Each of these graphs present in the plane (V, λ_{flight}) ($\lambda = M\bar{\lambda}$, where $\bar{\lambda} = 1/(\mu\chi_\alpha r_\alpha)$ is the scaling factor), the dangerous and undangerous portions of the flutter boundary for open/closed loop sectional wings. The corresponding Liapunov quantity, is depicted in Figs. 11, 13, 15, in the plane (L, λ_{flight}). Moreover, in Figs. 10 through 16 aerodynamic and physical hard nonlinearities have been included $\delta_A = 1$, $\delta_S = 1$; $B = 50$. With dotted lines are marked the values of the flight Mach number where the transition from the benign to the catastrophic character of the flutter boundary occurs. As a consequence, a complete picture of the variation of dangerous and benign parts of the flutter boundary has been provided. In the plots depicting the Liapunov quantity, the gain parameters ψ_i ($i=1,2$), help to understand the potentiality of the linear and nonlinear active control to enhance the flutter instability behavior and convert the dangerous flutter boundary into an undangerous one.

Notice that, the linear active control is able to act also toward the enhancement of the flutter boundary. This can be readily seen either from Eq. (27) and from Figs. 3 and 5 where for $\psi_1 \neq 0$, V_F was depicted, and the beneficial influence on the increase of the flutter speed revealed.

The dangerous and undangerous portions of the flutter boundary for open/closed loop sectional wings via the use of the two different aerodynamic theories (PTA and SWT) are presented in Fig. 16. In addition to what was stated before about these two theories, from this plot and from Table 1, it can be revealed that the PTA gives more conservative results (less then 3% difference at the transition flight Mach number), as compared with the SWT, in the sense that within PTA the transition from the benign to catastrophic flutter boundary appears at slightly lower flight Mach numbers as compared with those featured by SWT. This conclusion was expected by comparing the cubic nonlinearities in the two pressure expressions (see Eqs. (10) and (12)), wherefrom it clearly appears that the one within the PTA is larger than that in SWT.

Conclusions

It was shown that in some circumstance the hard physical and aerodynamic nonlinearities contribute in different manners to the determination of the "undangerous" or "dangerous" character of the flutter critical boundary, in the sense that the "hard" nonlinearities render the flutter boundary benign, whereas the "soft" ones contribute to its catastrophic character. In addition, at high flight Mach numbers the aerodynamic nonlinearities contribute invariably to the "dangerous" character of the flutter boundary. This implies that, with the increase of the hypersonic flight speed, when the aerodynamic nonlinearities become prevalent, the flutter boundary will become catastrophic, irrespective of the presence of hard physical nonlinearities.

On the other hand, soft physical nonlinearities $(B<0)$ contribute in the same sense, as the aerodynamic nonlinearities, to the dangerous character of the flutter boundary. It was also shown that, in the case when due to the nature of the involved nonlinearities, when the catastrophic aeroelastic failure can occur, an active control can be used as to convert the flutter boundary in a benign one or to shift the transition between these two states toward larger flight Mach numbers.

Numerical simulations illustrate that: i) the increase of the values of the active control gains yields an increase of the "undangerous" portions of the flutter instability boundary, ii) with the increase of the supersonic flight Mach numbers that results in an increase of aerodynamic nonlinearities, a decrease of the "undangerous" portions of the flutter instability boundary is experienced, iii) in the cases in which catastrophic aeroelastic failures can be experienced, the active control capabilities can render the flutter boundary safe, in the sense that its crossing does not yields a catastrophic failure, and iv) a comparisons of the results provided when PTA and the SWT are used, reveal that the PTA gives more conservative results.

As clearly appears from this paper, the issue of generating the active control moment was not addressed. It is in the authors' believe that this can be produced via a device operating similarly to a spring, whose linear and nonlinear characteristics can be controlled.

To the best of the authors' knowledge, this is the first paper where the problem of the character of the flutter boundary of cross-sectional wing was approached in a so general context, in the sense that, the implications of the various nonlinearities considered in conjunction with the presence of a control capabilities have been considered together as to analyze this problem, and determine also the combination of those nonlinearities and parameters that can yield a conversion of the catastrophic type of flutter into a benign one. Needless to say, the concept and methodology presented here can be extended as to treat more complex associated problems involving 3-D straight and swept aircraft wings.

Acknowledgment

The support of this research by the NASA Langley Research Center through Grants NAG-1-2281 and NAG-1-01007 is acknowledged. Piergiovanni Marzocca would like also to acknowledge the advice supplied by Prof. G. Chiocchia from the Politecnico di Torino, Aeronautical and Space Department, Turin, Italy.

References

[1] Librescu, L., "Aeroelastic Stability of Orthotropic Heterogeneous Thin Panels in the Vicinity of the Flutter Critical Boundary," *Journal de Mécanique*, Part I, Vol. 4, No. 1, 1965, pp. 51-76; Part II, Vol. 6, No. 1, 1967, pp. 133-152.

[2] Librescu, L., *Elastostatics and Kinetics of Anisotropic and Heterogeneous Shell-Type Structures*, Aeroelastic Stability of Anisotropic Multilayered Thin Panels, Noordhoff Internat. Publ., Leyden, The Netherlands, 1975, pp. 106-158.

[3] Lee, B. H. K., Price, S. J., and Wong, Y. S., "Nonlinear Aeroelastic Analysis of Airfoils: Bifurcation and Chaos," *Progress in Aerospace Sciences*, Vol. 35, 1999, pp. 205-334.

[4] Breitbach, E. J., "Effects of Structural Nonlinearities on Aircraft Vibration and Flutter," AGARD TR, Vol. 665, 1977, and on *34th Structures and Materials AGARD Panel Meeting*, Voss, Norway, AGARD Report 554.

[5] Price, S. J., Alighanbari, H., and Lee, B. H. K., "The Aeroelastic Response of a Two-Dimensional Airfoil with Bilinear and Cubic Structural Nonlinearities," *Journal of Fluid and Structures*, Vol. 9, 1995, pp. 175-193, presented as AIAA Paper 94-154 at the *AIAA/ASME/ ASCE/AHS/ASC 35th Structures, Structural Dynamics and Materials Conference*, AIAA, Washington, DC, 1994, pp. 1771-1780.

[6] Lee, B. H. K., and Desrochers, J., "Flutter Analysis of a Two-dimensional Airfoil Containing Structural Nonlinearities," National Research Council of Canada, Aeronautical Report LR-618, Ottawa, Canada (1987).

[7] O'Neil, T., and Strganac, T. W., "Aeroelastic response of a rigid wing supported by nonlinear springs," *Journal of Aircraft*, Vol. 35 No. 4, 1998, p. 616-622.

[8] Chandiramani, N. K., Librescu, L., and Plaut, R., "Flutter of Geometrically Imperfect Shear-Deformable Laminated Flat Panels Using Non-Linear Aerodynamics," *Journal of Sound and Vibration*, Vol. 192, No. 1, 1996, pp. 79-100.

[9] Namachivaya, N. S., and Lee, A., "Dynamics of Nonlinear Aeroelastic Systems," Vol. AD 53, No. 3, *4th International Symposium on Fluid-Structure Interaction, Aeroelasticity, Flow-Induced Vibration and Noise*, ASME, 1997, pp. 165-173.

[10] Mastroddi, F., and Morino, L., "Limit-Cycle Taming by Nonlinear Control with Application to Flutter," *The Aeronautical Journal*, Vol. 100, No. 999, 1996, pp. 389-396.

[11] Ko, J., Kurdila, A. J., and Strganac, T. W., "Nonlinear Control Theory for a Class of Structural Nonlinearities in a Prototypical Wing Section," *Journal of Guidance, Control, and Dynamics*, Vol. 20, No. 6, 1997, pp. 1181-1189.

[12] Ko, J., Strganac, T.W., and Kurdila, A.J., "Stability and Control of a Structurally Nonlinear Aeroelastic System," *Journal of Guidance, Control and Dynamics*, Vol. 21, No. 5, 1998, pp. 718-725.

[13] Strganac, T. W., Ko, J., Thompson, D. E., and Kurdila, A. J., "Identification and Control of Limit Cycle Oscillations in Aeroelastic Systems," *Journal of Guidance, Control, and Dynamics*, Vol. 23, No. 6, 2000, pp. 1127-1133.

[14] Librescu, L., and Na, S. S., "Bending Vibration Control of Cantilevers Via Boundary Moment and Combined Feedback Control Laws," *Journal of Vibration and Controls*, Vol. 4, No. 6, 1998, pp. 733-746.

[15] Song, O., Librescu, L., and Rogers, C. A., "Application of Adaptive Technology to Static Aeroelastic Control of Wing Structures," *AIAA Journal*, Vol. 30, No. 12, 1992, pp. 2882-2889.

[16] Bautin, N. N., *The Behaviour of Dynamical Systems Near the Boundaries of the Domain of Stability*, Nauka, Moskva, 2nd ed., 1984, (In Russian).

[17] Dessi, D., Mastroddi, F., and Morino, L., "Limit-Cycle Stability Reversal Near a Hopf Bifurcation with Aeroelastic Applications," *Journal of Sound and Vibration*, in press.

[18] Hopf, E., Bifurcation of a Periodic Solution from a Stationary Solution of a System of Differential Equations, *Ber. Math. Phys. Klasse*, Sächsischen Acad. Wiss. Leipzig (Germany), Vol. XCIV, 1942, pp. 3-32.

[19] Zhao, L. C., and Yang, Z. C., "Chaotic Motions of an Airfoil with Non-Linear Stiffness in Incompressible Flow," *Journal of Sound and Vibration*, Vol. 138, 1990, pp. 245-254.

[20] Bisplinghoff, R. L., and Ashley, H. *Principles of Aeroelasticity*, Dover Publications, Inc., 1996.

[21] Ashley, H., and Zartarian, G., "Piston Theory – A New Aerodynamic Tool for the Aeroelastician," *Journal of Aeronautical Science*, Vol. 23, 1956, pp. 1109-1118.

[22] Lighthill, M. J., "Oscillating Airfoils at High Mach Numbers," *Journal of Aeronautical Science*, Vo. 20, No. 6, 1953, pp. 402-406.

[23] Librescu, L., Aeroelasticity, Course Notes, VPI, 2000.

[24] Carafoli, E., and Berbente, C., "Determination of Pressure and Aerodynamic Characteristics of Delta Wings in Supersonic – Moderate Hypersonic Flow," Revue Roumaine des Sciences Techniques. Serie de Mecanique Appliquee, Vol. 11, No. 3, 1866, pp. 587-613.

[25] Carafoli, E., *Wing Theory in Supersonic Flow*, International Series on Monographs in Aeronautics and Astronautics, Vol. 7, Pergamon Press, 1969.

[26] Malkin, I. G., *Theory of Stability of Motion*, Translation Series, AEC-tr-3352, *Physics and Mathematics*, 1963, pp. 178-184.

[27] Liapunov, A. M., *General Theory of the Stability of Motion*, Izd., Moskva, 1950, English translation by Academic Press, New York, 1966.

Appendix A

The coefficients of the aeroelastic governing system represented in state-space form, Eqs. (21):

$$a_1^{(3)} = -\frac{\varpi^2 r_\alpha^2}{V^2\left(r_\alpha^2 - \chi_\alpha^2\right)}, \tag{A.1}$$

$$a_2^{(3)} = \frac{M_\infty \mu \chi_\alpha r_\alpha^2 (1+\psi_1) - V^2\gamma\left[(x_0 - 1)\chi_\alpha + r_\alpha^2\right]}{V^2 M_\infty \mu\left(r_\alpha^2 - \chi_\alpha^2\right)}, \tag{A.2}$$

$$\delta_A a_{222}^{(3)} = -\frac{M_\infty (1+\kappa)\gamma^3\left[(x_0 - 1)\chi_\alpha + r_\alpha^2\right]}{12\mu\left(r_\alpha^2 - \chi_\alpha^2\right)}, \tag{A.3}$$

$$\delta_S a_{222}^{(3)} = B\frac{\chi_\alpha r_\alpha^2}{V^2\left(r_\alpha^2 - \chi_\alpha^2\right)}, \tag{A.4}$$

$$\delta_C a_{222}^{(3)} = \psi_2 \frac{\chi_\alpha r_\alpha^2}{V^2\left(r_\alpha^2 - \chi_\alpha^2\right)}, \tag{A.5}$$

$$a_3^{(3)} = -\frac{2M_\infty \mu \varpi \zeta_h r_\alpha^2 + V\gamma\left[(x_0 - 1)\chi_\alpha + r_\alpha^2\right]}{VM_\infty \mu\left(r_\alpha^2 - \chi_\alpha^2\right)}, \tag{A.5}$$

$$a_4^{(3)} = \frac{V\gamma\left[\left(3x_0^2 - 6x_0 + 4\right)\chi_\alpha + 3(x_0 - 1)r_\alpha^2\right] + 6M_\infty \mu \zeta_\alpha \chi_\alpha r_\alpha^2}{3VM_\infty \mu\left(r_\alpha^2 - \chi_\alpha^2\right)}, \tag{A.6}$$

$$a_1^{(4)} = \frac{\varpi^2 \chi_\alpha}{V^2\left(r_\alpha^2 - \chi_\alpha^2\right)}, \tag{A.7}$$

$$a_2^{(4)} = \frac{V^2\gamma(x_0 - 1 + \chi_\alpha) - M_\infty \mu r_\alpha^2 (1+\psi_1)}{V^2 M_\infty \mu\left(r_\alpha^2 - \chi_\alpha^2\right)}, \tag{A.8}$$

$$\delta_S a_{222}^{(4)} = -B\frac{r_\alpha^2}{V^2\left(r_\alpha^2 - \chi_\alpha^2\right)}, \tag{A.9}$$

$$\delta_C a_{222}^{(4)} = -\psi_2 \frac{r_\alpha^2}{V^2\left(r_\alpha^2 - \chi_\alpha^2\right)}, \tag{A.9}$$

$$\delta_A a_{222}^{(4)} = \frac{\lambda^3 M_\infty (1+\gamma)(x_0 - 1 + \chi_\alpha)}{12\mu\left(r_\alpha^2 - \chi_\alpha^2\right)}, \tag{A.10}$$

$$a_3^{(4)} = \frac{V\lambda(x_0 - 1 + \chi_\alpha) + 2M_\infty \mu \varpi \zeta_h \chi_\alpha}{VM_\infty \mu\left(r_\alpha^2 - \chi_\alpha^2\right)}, \tag{A.11}$$

$$a_4^{(4)} = -\frac{V\lambda\left[\left(3x_0^2 - 6x_0 + 4\right) + 3(x_0 - 1)\chi_\alpha\right] + 6M_\infty \mu r_\alpha^2 \zeta_\alpha}{3VM_\infty \mu\left(r_\alpha^2 - \chi_\alpha^2\right)}, \tag{A.12}$$

Figure Captions

Figs. 1a and 1b: Character of the flutter boundary in the terms of *LCOs* amplitudes – V_F flutter speed of the linear system; H-B: Hopf-Bifurcation.

Fig. 2: Comparison of the predictions of the flutter speed vs. the flight Mach number when using Piston Theory Aerodynamics (PTA), of aerodynamics based on Shock Waves Theory (SWT), and of exact unsteady supersonic aerodynamics,

($\mu = 100; \chi_\alpha = 0.25; \overline{\omega} = 1.2; r_\alpha = 0.5; \zeta_\alpha = \zeta_h = 0; x_0 = 0.5$).

Fig. 3: Flutter speed vs. flight Mach number. Influence of the linear control gain ψ_1.

Figs. 4a and **4.b:** Generic representation of the dangerous and undangerous portion of the flutter critical boundary. The upper plot (4.a) is in the ($V - M_{flight}$) plane, while the bottom one (4.b) is in the ($L - M_{flight}$) plane; $L < 0$ correspond to $V_r > V_F$ and vice versa.

Fig. 5: Evaluation of the flutter speed for selected flight Mach numbers vs. linear control gain ψ_1.

Fig. 6: Influence of the physical and aerodynamical nonlinearities on the First Liapunov Quantity L for the uncontrolled cross-sectional wing.

Fig. 7: Influence of the physical nonlinearities on the First Liapunov Quantity L in the presence/absence of linear and nonlinear active control gains. Aerodynamic nonlinearities retained. Flutter character change for system encompassing physical hard nonlinearity.

Fig. 8: Conversion from subcritical to supercritical H-B via nonlinear active control, for system encompassing physical soft nonlinearity $(B = -10)$.

Fig. 9: Subcritical H-B for system encompassing physical soft nonlinearity $(B = -10)$, linear active control included.

Fig. 10: Undangerous and dangerous portions of the flutter critical boundary in the presence of linear control.

Fig. 11: Influence of the linear control on the First Liapunov Quantity L.

Fig. 12: Undangerous and dangerous portions of the flutter critical boundary in the presence of nonlinear control.

Fig. 13: Influence of the nonlinear control on the First Liapunov Quantity L.

Fig. 14: Undangerous and dangerous portions of the flutter critical boundary in the presence of linear and nonlinear controls.

Fig. 15: Influence of the linear and nonlinear controls on the First Liapunov Quantity L.

Fig. 16: Undangerous and dangerous portions of the flutter critical boundary with and without control in presence of both nonlinearities. Comparison between SWT and PTA.

Table

Tab. 1: Undangerous and dangerous portions of the flutter critical boundary for PTA and SWT.

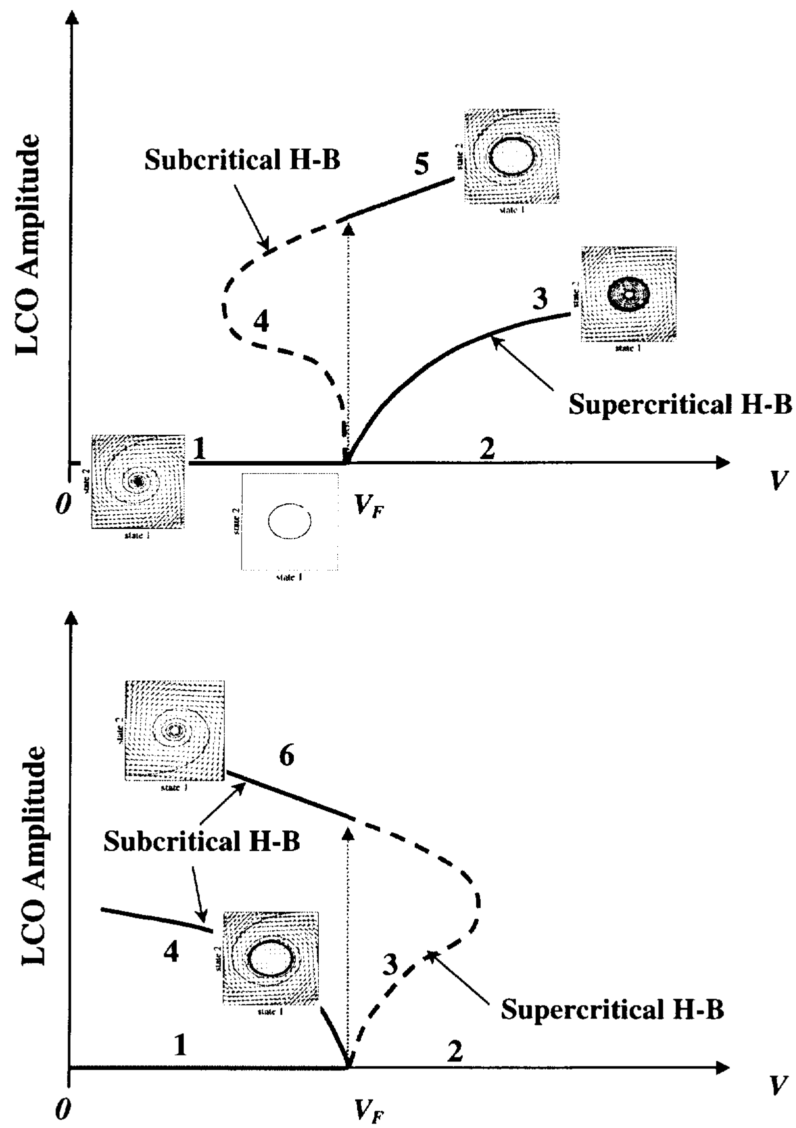
LCO Amplitude
Subcritical H-B
5
4
3
Supercritical H-B
1
2
0
V_F
V
LCO Amplitude
6
Subcritical H-B
4
3
Supercritical H-B
1
2
0
V_F
V

Fig. 1.a and 1.b

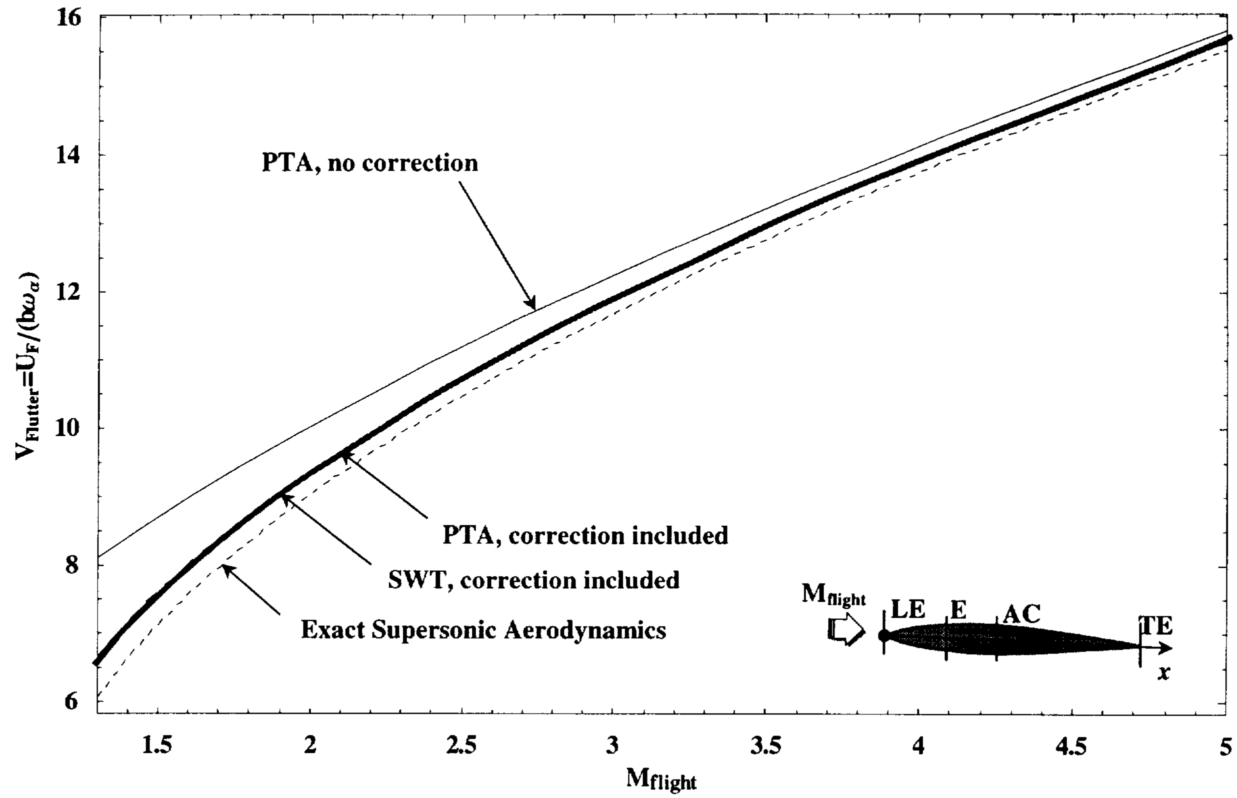

16
14
12
10
8
6
1.5
2
2.5
3
3.5
4
4.5
5
$V_{Flutter}=U_F/(b\omega_\alpha)$
M_{flight}
PTA, no correction
PTA, correction included
SWT, correction included
Exact Supersonic Aerodynamics
M_{flight}
LE
E
AC
TE
x

Fig. 2

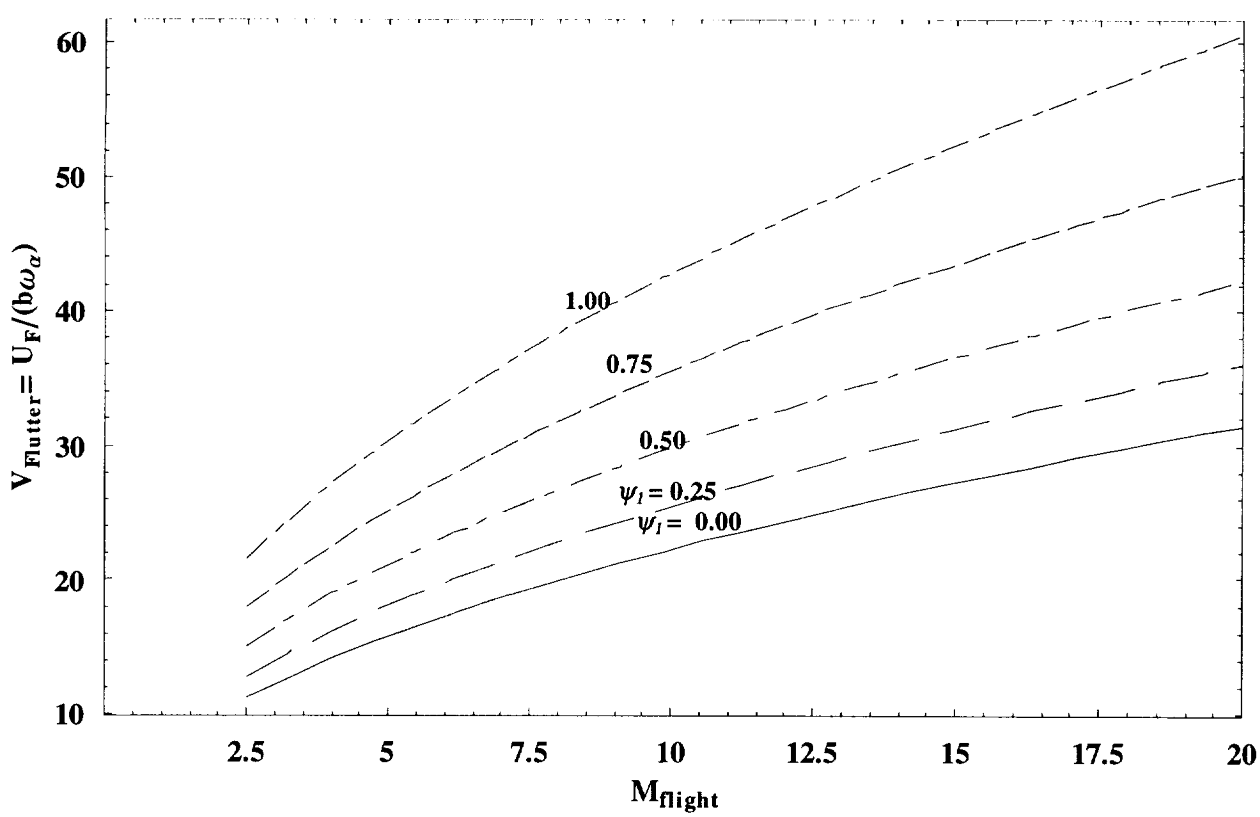

60
50
40
30
20
10
2.5
5
7.5
10
12.5
15
17.5
20
$V_{Flutter}= U_F/(b\omega_\alpha)$
M_{flight}
1.00
0.75
0.50
$\psi_1 = 0.25$
$\psi_1 = 0.00$

Fig. 3

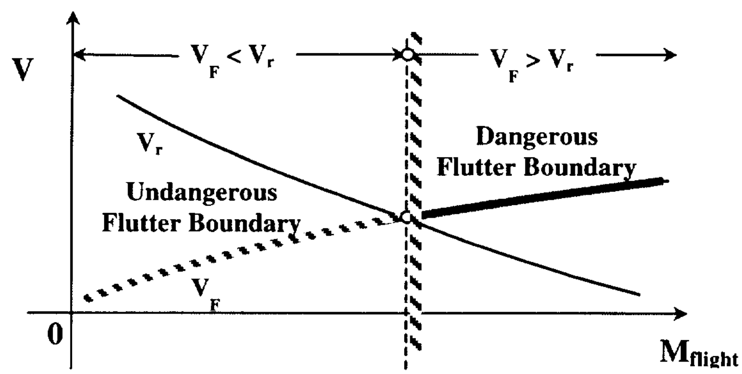
V
$V_F < V_r$
$V_F > V_r$
V_r
Dangerous
Flutter Boundary
Undangerous
Flutter Boundary
V_F
0
M_{flight}

Fig. 4a

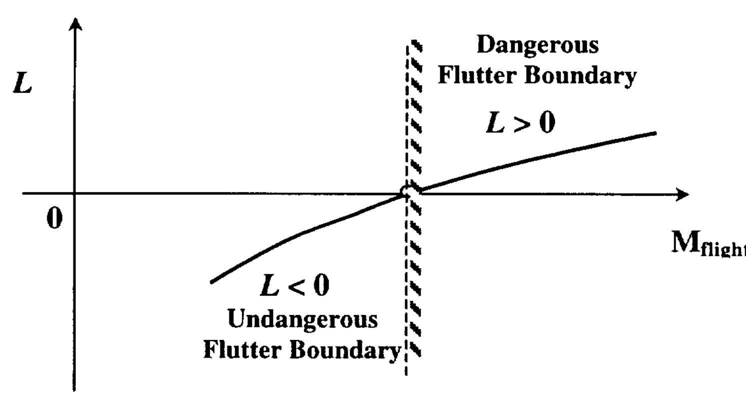
L
Dangerous
Flutter Boundary
$L > 0$
0
M_{flight}
$L < 0$
Undangerous
Flutter Boundary

Fig. 4b

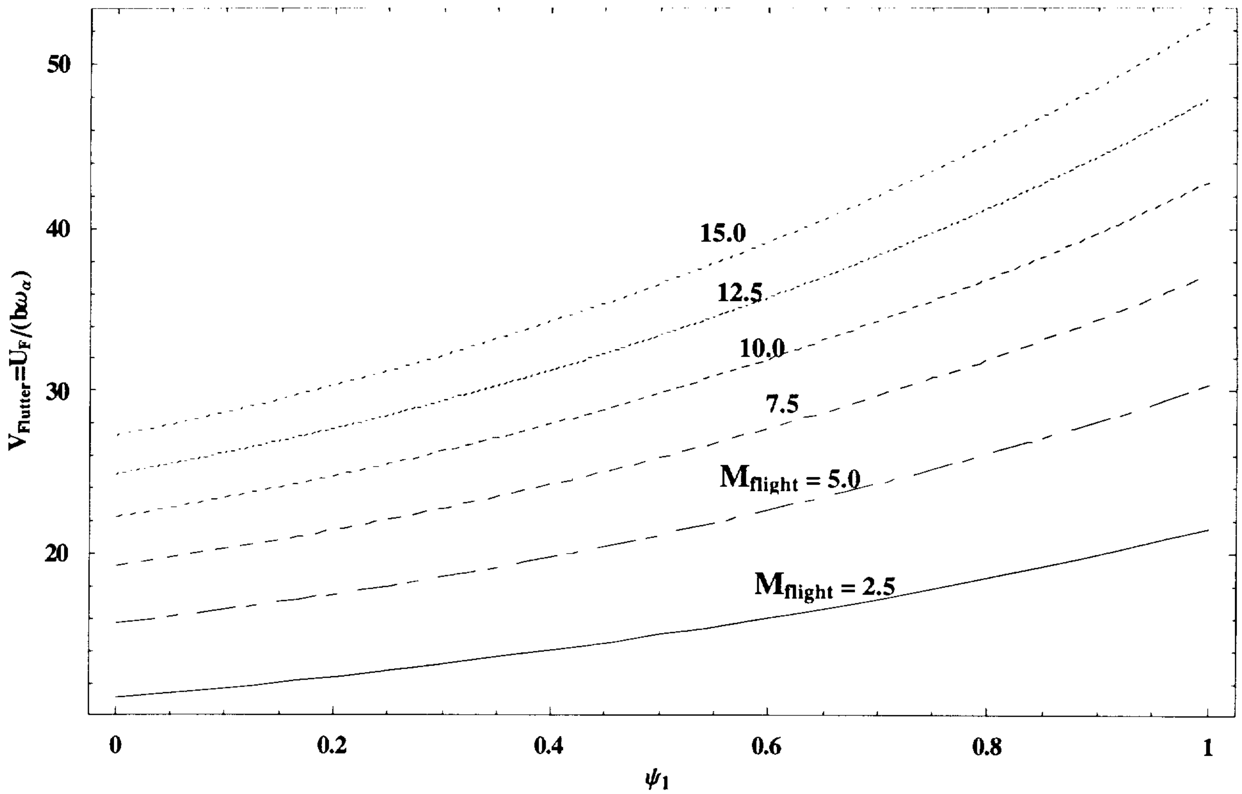

50
40
30
20
$V_{Flutter}=U_F/(b\omega_\alpha)$
15.0
12.5
10.0
7.5
M_{flight} = 5.0
M_{flight} = 2.5
0
0.2
0.4
0.6
0.8
1
ψ_1

Fig. 5

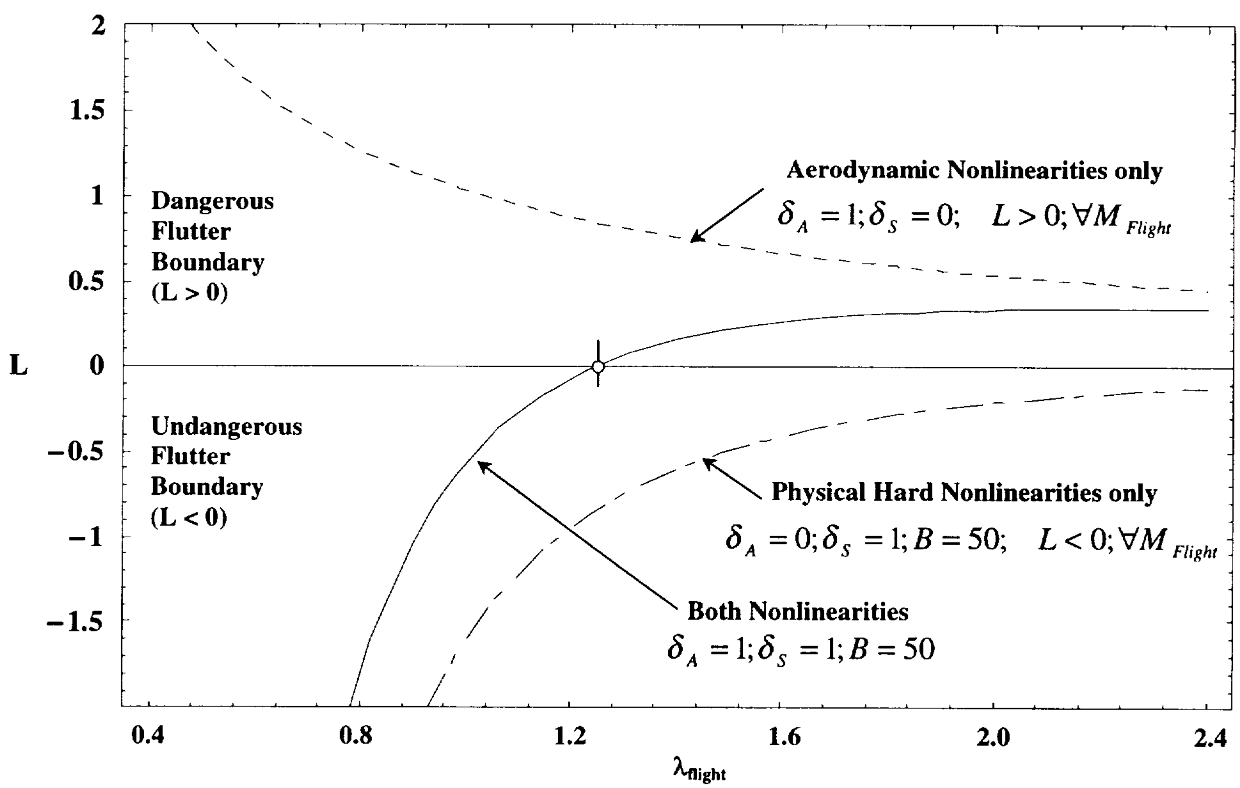

2
1.5
1
0.5
L
0
−0.5
−1
−1.5
Dangerous Flutter Boundary (L > 0)
Undangerous Flutter Boundary (L < 0)
Aerodynamic Nonlinearities only
$\delta_A = 1; \delta_S = 0; \quad L > 0; \forall M_{Flight}$
Physical Hard Nonlinearities only
$\delta_A = 0; \delta_S = 1; B = 50; \quad L < 0; \forall M_{Flight}$
Both Nonlinearities
$\delta_A = 1; \delta_S = 1; B = 50$
0.4
0.8
1.2
1.6
2.0
2.4
λ_{flight}

Fig. 6

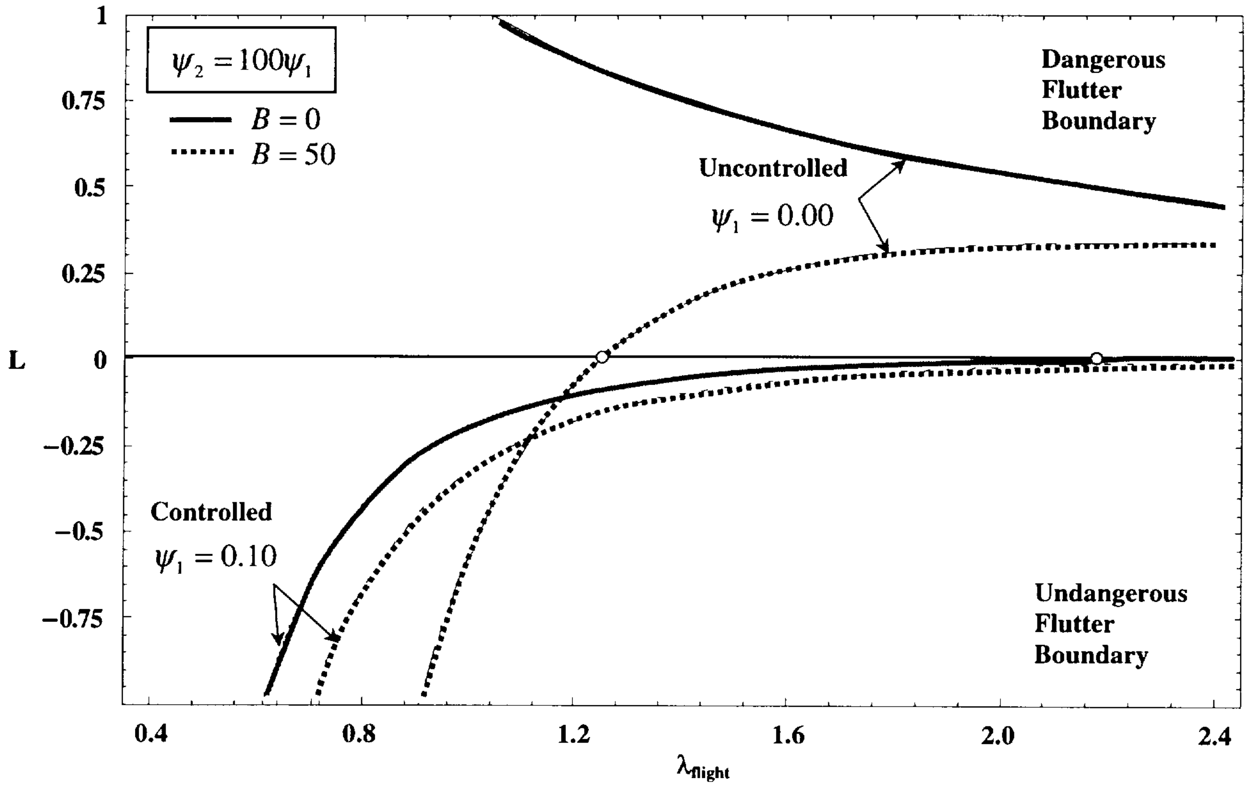
$\psi_2 = 100\psi_1$
$B = 0$
$B = 50$
Dangerous Flutter Boundary
Uncontrolled
$\psi_1 = 0.00$
Controlled
$\psi_1 = 0.10$
Undangerous Flutter Boundary
L
1
0.75
0.5
0.25
0
−0.25
−0.5
−0.75
0.4
0.8
1.2
1.6
2.0
2.4
λ_{flight}

Fig. 7

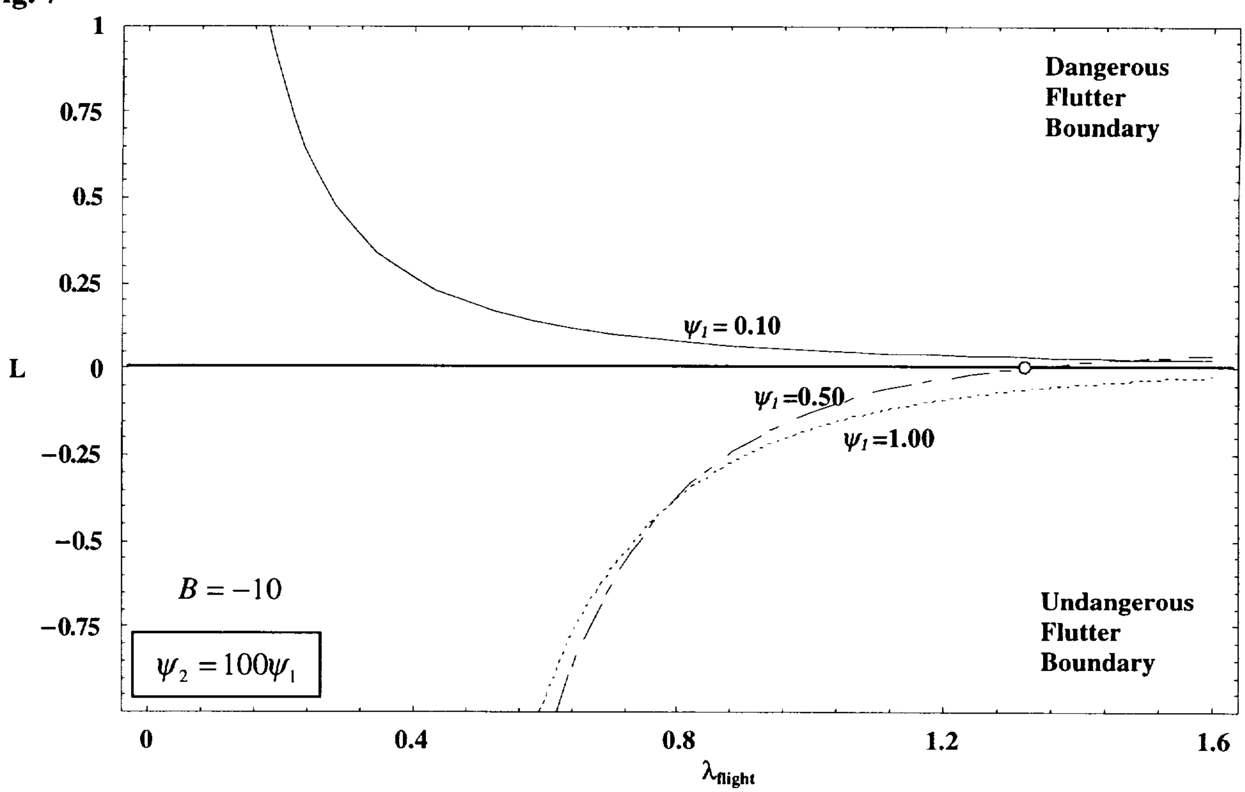
Dangerous Flutter Boundary
$\psi_1 = 0.10$
$\psi_1 = 0.50$
$\psi_1 = 1.00$
$B = -10$
$\psi_2 = 100\psi_1$
Undangerous Flutter Boundary
L
1
0.75
0.5
0.25
0
−0.25
−0.5
−0.75
0
0.4
0.8
1.2
1.6
λ_{flight}

Fig. 8

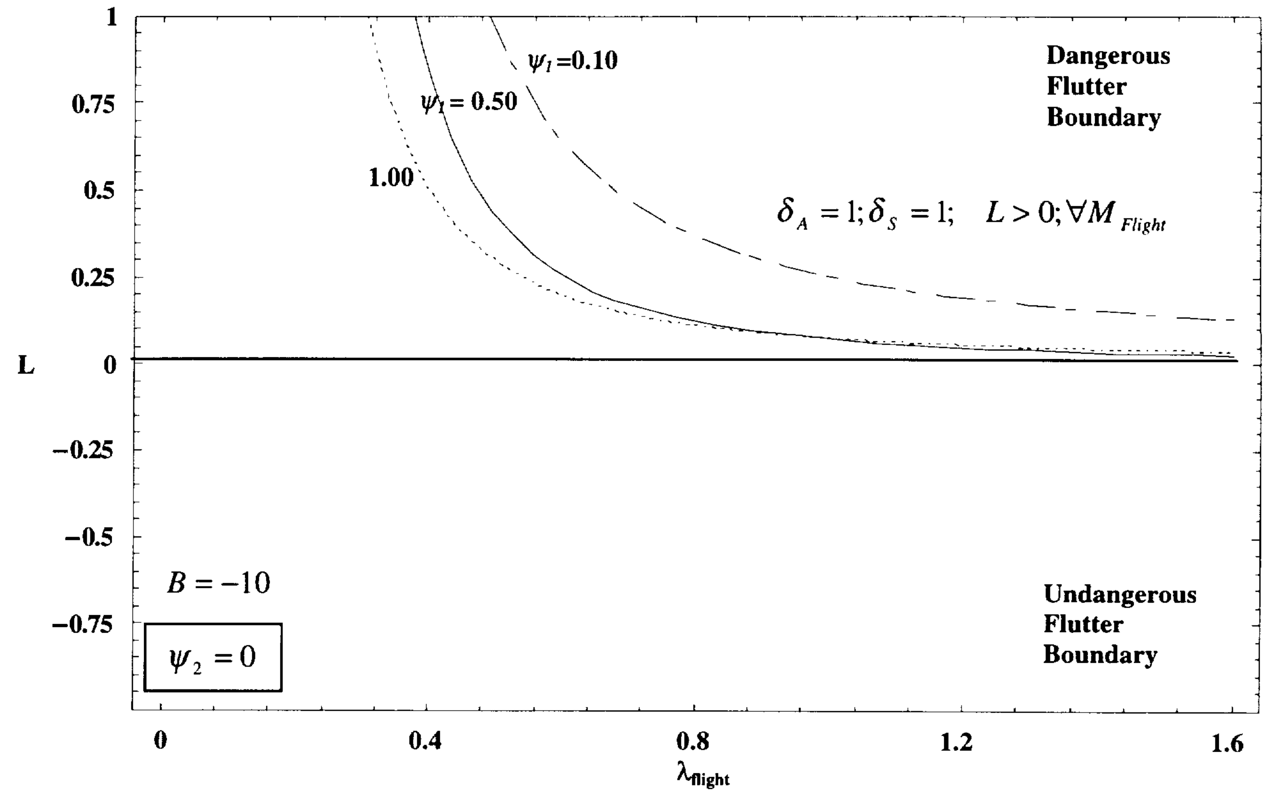

1
0.75
0.5
0.25
L
0
−0.25
−0.5
−0.75
ψ_1 =0.10
ψ_1 = 0.50
1.00
Dangerous
Flutter
Boundary
$\delta_A = 1; \delta_S = 1; \quad L > 0; \forall M_{Flight}$
$B = -10$
$\psi_2 = 0$
Undangerous
Flutter
Boundary
0
0.4
0.8
1.2
1.6
λ_{flight}

Fig. 9

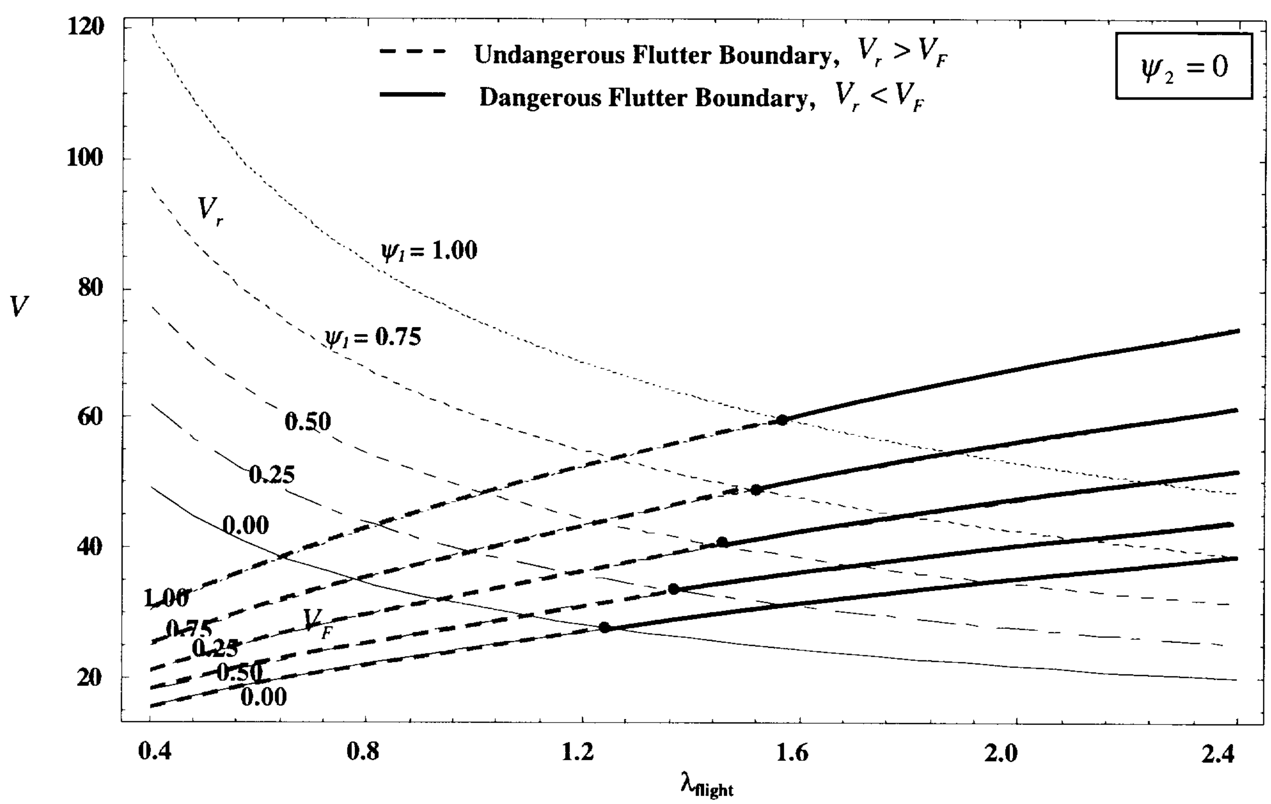

Undangerous Flutter Boundary, $V_r > V_F$
Dangerous Flutter Boundary, $V_r < V_F$
$\psi_2 = 0$
120
100
80
V
60
40
20
V_r
ψ_1 = 1.00
ψ_1 = 0.75
0.50
0.25
0.00
1.00
0.75
0.25
0.50
0.00
V_F
0.4
0.8
1.2
1.6
2.0
2.4
λ_{flight}

Fig. 10

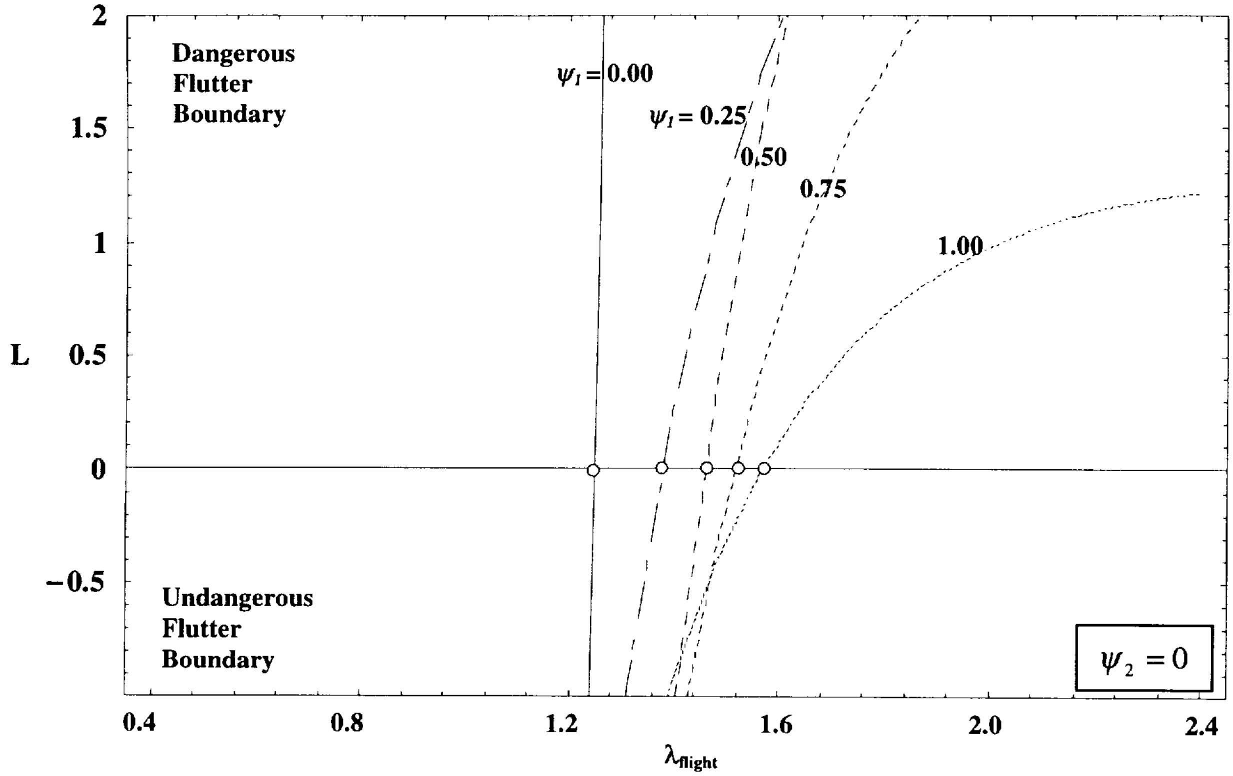
Dangerous
Flutter
Boundary
Undangerous
Flutter
Boundary
ψ1 = 0.00
ψ1 = 0.25
0.50
0.75
1.00
ψ2 = 0
L
2
1.5
1
0.5
0
−0.5
0.4
0.8
1.2
1.6
2.0
2.4
λflight

Fig. 11

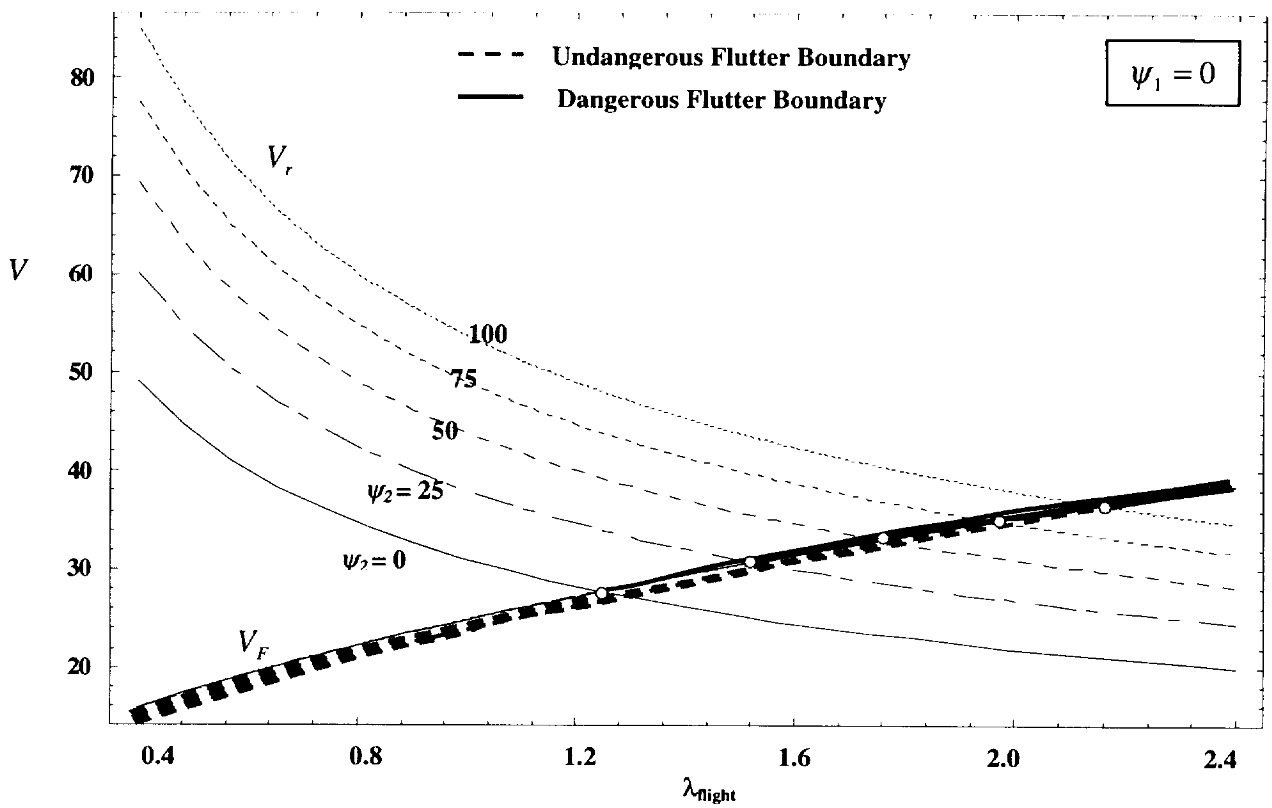
Undangerous Flutter Boundary
Dangerous Flutter Boundary
ψ1 = 0
V
Vr
VF
100
75
50
ψ2 = 25
ψ2 = 0
80
70
60
50
40
30
20
0.4
0.8
1.2
1.6
2.0
2.4
λflight

Fig. 12

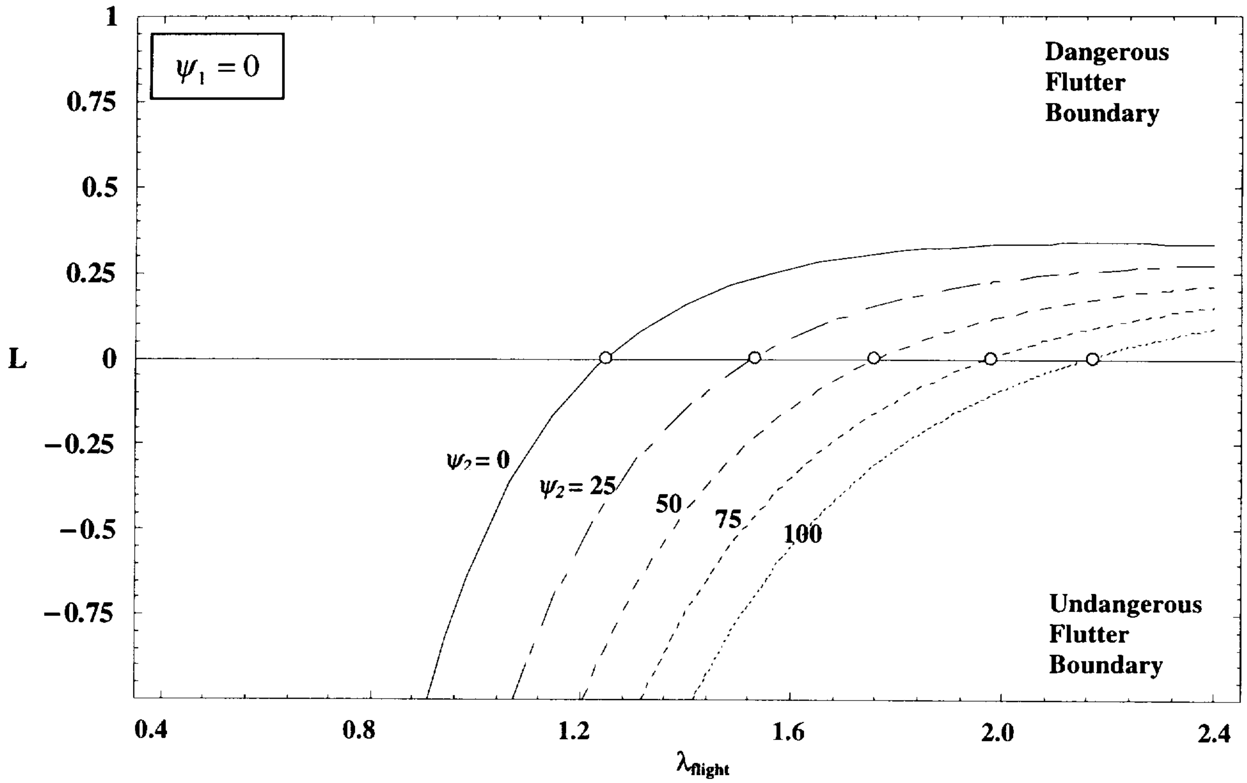

$\psi_1 = 0$
Dangerous Flutter Boundary
Undangerous Flutter Boundary
$\psi_2 = 0$
$\psi_2 = 25$
50
75
100
L
λ_{flight}

Fig. 13

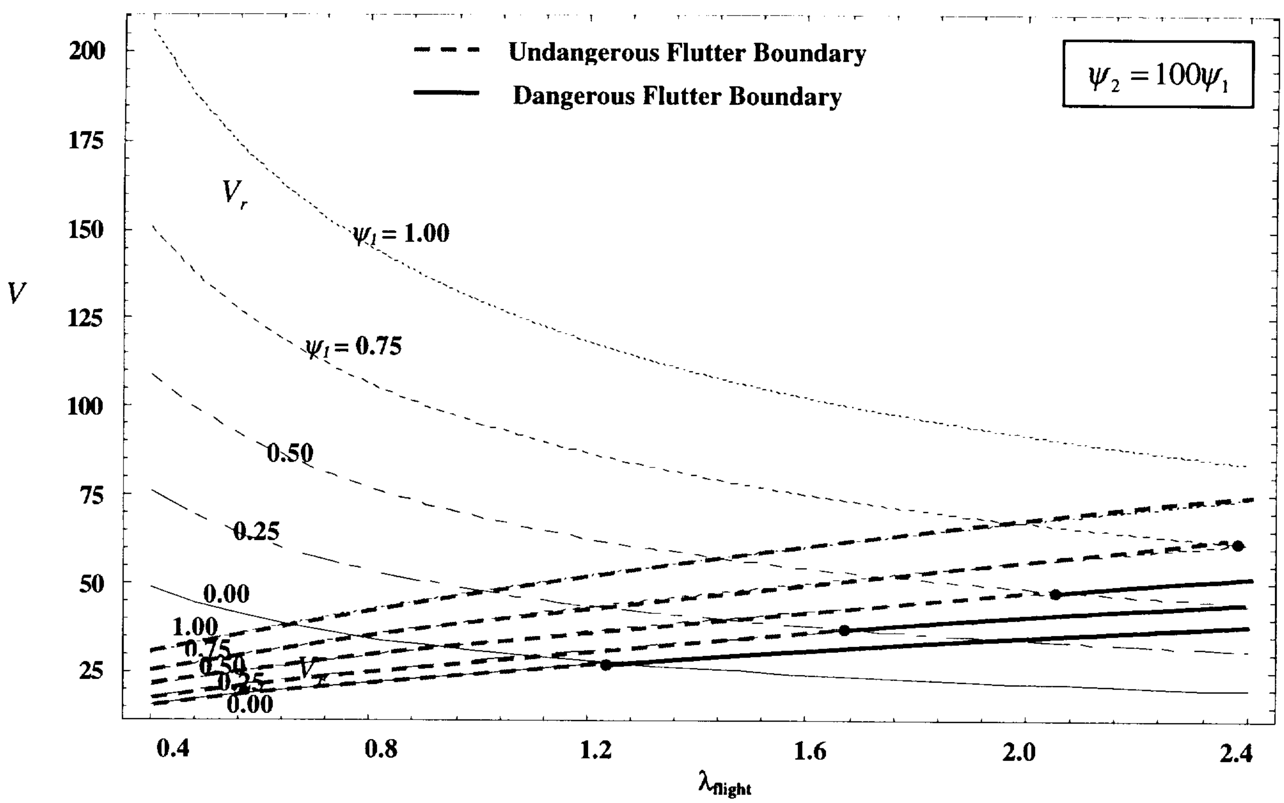

Undangerous Flutter Boundary
Dangerous Flutter Boundary
$\psi_2 = 100\psi_1$
V_r
$\psi_1 = 1.00$
$\psi_1 = 0.75$
0.50
0.25
0.00
1.00
0.75
0.50
0.25
0.00
V_F
V
λ_{flight}

Fig. 14

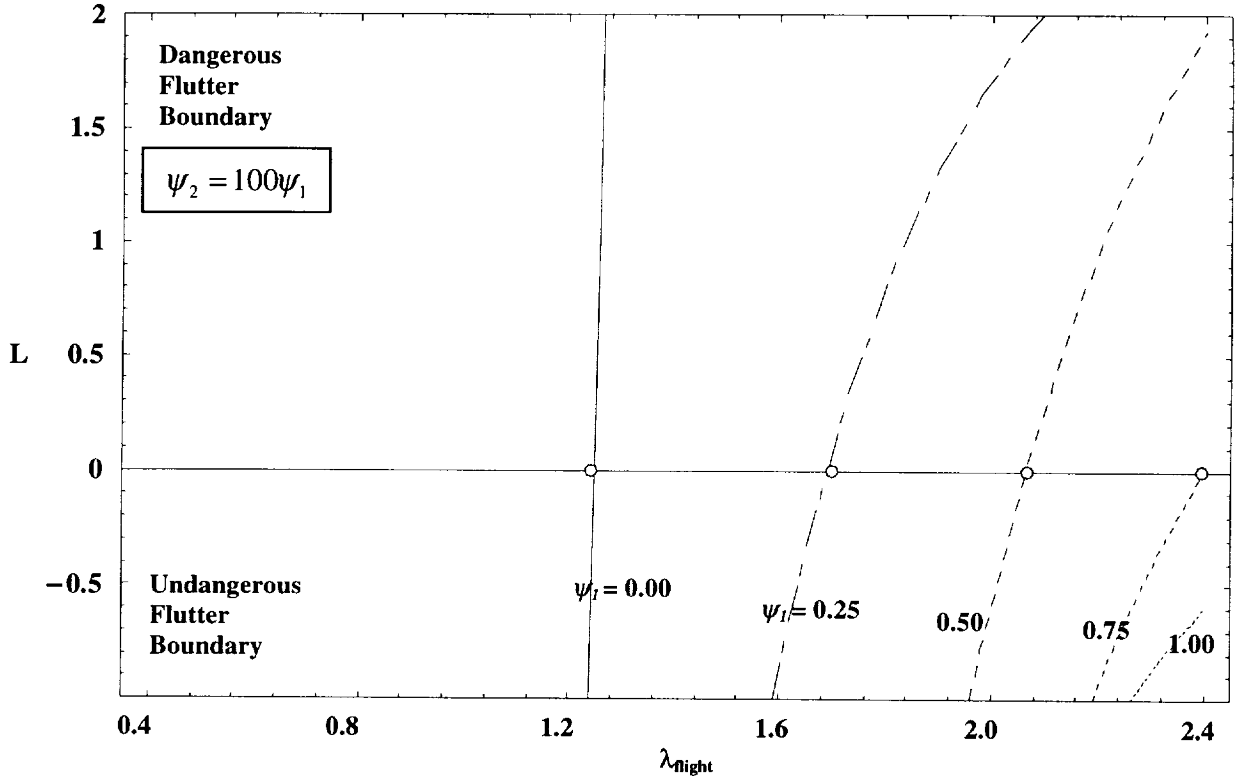

Dangerous
Flutter
Boundary
$\psi_2 = 100\psi_1$
L
Undangerous
Flutter
Boundary
$\psi_1 = 0.00$
$\psi_1 = 0.25$
0.50
0.75
1.00
λ_{flight}

Fig. 15

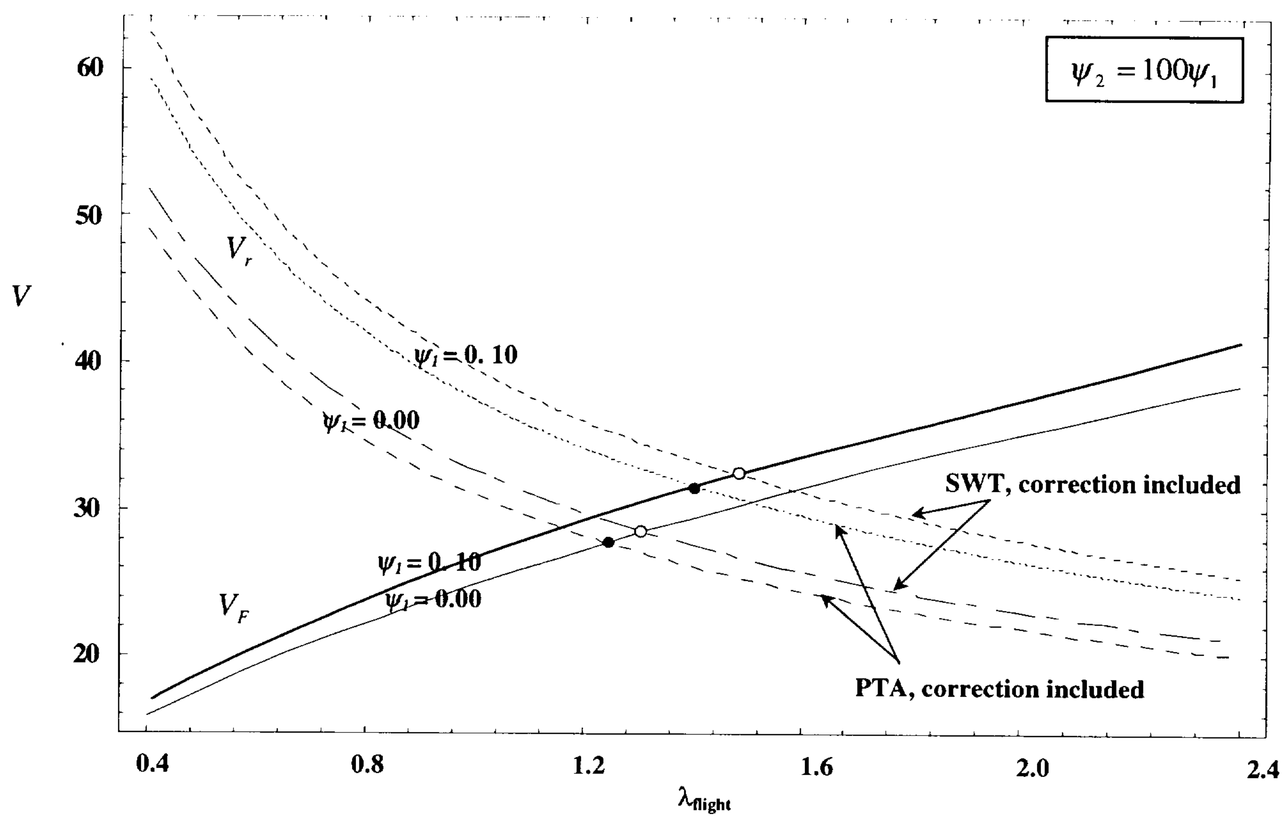

$\psi_2 = 100\psi_1$
V
V_r
$\psi_1 = 0.10$
$\psi_1 = 0.00$
SWT, correction included
$\psi_1 = 0.10$
$\psi_1 = 0.00$
V_F
PTA, correction included
λ_{flight}

Fig. 16

λ_{flight}	$\lambda_{Flutter}$	λ_r - PTA	λ_r - SWT	$10^{10}\,L$ - PTA		$10^{10}\,L$ - SWT	
1.200	2.182	2.263	2.386	-6.679		-15.437	
1.208	2.189	2.256	2.378	-5.402		-14.107	
1.216	2.196	2.248	2.370	-4.164		-12.817	
1.224	2.203	2.241	2.362	-2.965	Undangerous Flutter Boundary	-11.566	
1.232	2.211	2.234	2.355	-1.803		-10.352	
1.240	**2.218**	**2.226**	2.347	**-0.676**		-9.175	
1.248	**2.225**	**2.219**	2.339	**0.416**		-8.033	
1.256	2.232	2.212	2.332	1.474		-6.925	Undangerous Flutter Boundary
1.264	2.239	2.205	2.325	2.501		-5.849	
1.272	2.246	2.198	2.317	3.496		-4.806	
1.280	2.253	2.191	2.310	4.461		-3.793	
1.288	2.260	2.185	2.303	5.396		-2.811	
1.296	2.267	2.178	2.296	6.304	Dangerous Flutter Boundary	-1.857	
1.304	2.274	2.171	2.289	7.183		-0.930	
1.312	**2.281**	2.164	**2.282**	8.037		**-0.031**	
1.320	**2.288**	2.158	**2.275**	8.865		**0.842**	
1.328	2.295	2.151	2.268	9.668		1.689	
1.336	2.302	2.145	2.261	10.447		2.512	Dangerous Flutter Boundary
1.344	2.309	2.139	2.254	11.202		3.312	
1.352	2.316	2.132	2.248	11.935		4.088	
1.360	2.322	2.126	2.241	12.646		4.842	

Tab. 1